SOLUBILITY AND PSEUDO-POLYMORPHIC TRANSITIONS OF L-SERINE IN WATER-METHANOL SYSTEM

A Thesis
Presented to
The Academic Faculty

By

Chee-wei Jennifer Luk

In Partial Fulfillment
Of the Requirements for the Degree
Master of Science in Chemical Engineering

Georgia Institute of Technology

January 2005

SOLUBILITY AND PSEUDO-POLYMORPHIC TRANSITIONS OF L-SERINE IN WATER-METHANOL SYSTEM

Approved by:

Dr. Ronald W. Rousseau, Chair
School of Chemical and Biomolecular Engineering
Georgia Institute of Technology

Dr. Amyn S. Teja
School of Chemical and Biomolecular Engineering
Georgia Institute of Technology

Dr. Peter J. Ludovice
School of Chemical and Biomolecular Engineering
Georgia Institute of Technology

Date Approved: January 12, 2005

ACKNOWLEDGEMENT

I wish to take this opportunity to recognize several important people who have provided the support necessary for the completion of this research project. I would like to express my deepest gratitude to my thesis advisor, Dr. Ronald W. Rousseau, for his knowledge, guidance, and time provided during this research work. I appreciate the suggestions and remarks made by the committee members: Dr. Amyn S. Teja, and Dr. Peter J. Ludovice.

I would like to thank Dr. Wilkinson and his group members of the School of Chemistry and Biochemistry for help and for the use of the powder X-ray diffractometer.

I acknowledge past and present member of this research group for their valuable inputs, encouragement, and friendship: Karsten Bartling, Stephanie Barthe, Cosmas Bayuadri, Moussa Dikko, Daniel Euhus, Ana Fernandez, Young-soo Kim, Izumi Kurosawa, Jose Mendez del Rio, Laurent Nassif, and Jennifer Sherard.

I give my sincere thanks to all my friends, professors, and staff I met at Georgia Tech.

Finally and most importantly, I dedicate this thesis to my family whose love, continuous support, and faith in me has made this possible.

TABLE OF CONTENTS

LIST OF TABLES

LIST OF FIGURES

LIST OF ABBREVIATIONS

A	Integrated peak area in chromatogram
b	Constant in the linear equation used in HPLC calibration
C	Concentration of a solute in solution
D-	One form of stereoisomerism in which functional group is arranged around the chiral center carbon in anti-clockwise direction
DL-	Racemic mixture (optically inactive)
DL-Ser	DL-serine
HPLC	High performance liquid chromatography
hr	Hour
ICDD	International Centre for Diffraction Data
K	Constant in the linear equation used in HPLC calibration
K_s	Thermodynamic solubility constant for zwitterion
L-	One form of stereoisomerism in which functional group is arranged around the chiral center carbon in clockwise direction
L-Ser	L-Serine
M	Mass in grams
MeOH	Methanol
Min	Minutes
NRTL	Non random two liquid model
OPA	Ortho-phthaldialdehyde solution
P_c	Critical pressure
R	Ideal gas constant
t	time

T_c	Critical temperature
Tr	Reduced temperature, i.e. T_c/T
T_{tr}	Transition temperature
UNIFAC	Universal functional activity coefficient
XRD	X-ray diffraction
Z_{RA}	Modified Rackett equation input parameter
2θ	Bragg's angle
ρ	Saturated liquid density

SUMMARY

The research addressed in this thesis is focused on the solubility and pseudo-polymorphic transition of L-serine in mixed water-methanol systems. Cooling re-crystallizations were carried out that varied both temperature and methanol concentration. Solubilities were measured with high-performance liquid chromatography. It is found that the solubility increased with increase in temperature and decreased drastically with methanol concentration. The effect of temperature at which there is a transition of L-serine crystals from the rod-shaped (anhydrous) form to hexagonal (monohydrate) form was confirmed and that transition temperatures decreased with methanol concentrations in a non-linear manner. The solubility data were correlated and plotted using the van't Hoff equation and the enthalpy and entropy of dissolution were determined. These values increased with increase in methanol concentration. The solid crystals were analyzed by optical microscopy and powder X-ray diffraction. The rod-shaped crystals were identified to be anhydrous L-serine, while the hexagonal crystals were L-serine monohydrate. Dehydration of the monohydrated crystals in their solid-state was examined and the onset of such phenomenon was known to start once the crystals were removed from the solutions.

CHAPTER 1

INTRODUCTION

Amino acids have been important biochemical molecules in chemical, food, medical, and cosmetics industries. From the chemical industry standpoint, poly(amino acid)s are gaining attention as biodegradable polymers with their water-solubility. Examples of such polymers include poly(aspartic acid) (Roweton et al., 1997; Tachibana *et al*., 2003), poly(ε-L-lysine), and poly(γ-glutamic acid) (Obst and Steinbüchel, 2004; Kunioka, 2004). In the food industry, the total consumption of amino acids as dietary additives and beverages is estimated to be over 2 million tons (Kusomoto, 2001). Aspartame, the artificial sweetener, is the methyl ester of the dipeptide of amino acids aspartic acid and phenylalanine. Monosodium L-glutamate (MSG) is utilized as a flavor enhancer in various seasonings and processed foods. It is found that MSG produces a unique taste sensation, termed umami (Naim *et al*, 1991). Medically, amino acids are used in parenteral (Arii *et al*, 1994; Yamauchi *et al*., 2003) and enteral (Mazer *et al*. 2004) nutrition in patients to maintain basic nitrogen metabolism. Amino acids valine, isoleucine, glutamine, glutamic acid, and serine are therapeutic agents for treatment of ketosis (Kobayashi, 2003), a condition when the human's liver is depleted of the storage

glycogen. Amino acids also found wide application in the cosmetics industry. Examples include skin-moisturizing and wound-healing effects of mixtures with trehalose (Chikamatsu *et al*., 1994), anti-aging and environmental stress relieve of the skin promoted by amino acid derivatives such as N-capryloylglycine (Nagao *et al*., 2004), use of acetylmethionine and serine in hair-cleaning lotions (Suzuki *et al.,* 1974), and use of D-amino acids as odor-inhibiting ingredients in deodorants (Hayden *et al*., 2000).

Besides their commercial importance, amino acids share many similarities both chemically and physically with the more complex molecules such as peptides and proteins, as well as antibiotics and drugs (Nozaki and Tanford, 1971; Gekko, 1981; Hou and Poole, 1969). For example, amino acids exist as zwitterions in aqueous solutions at intermediate pH, which is also common for antibiotics.

Downstream processes in the pharmaceutical and biotechnology industries typically include solid-liquid separation, concentration, purification, washing, drying, and screening. These steps can take up as much as 50% of the production costs (Eyal and Bressler, 1993). Re-crystallization has been used as one of the most effective methods in purification because it does not require excessive heating. This method can be enhanced by addition of a second miscible solvent, called salting-out agent or anti-solvent, to drastically reduce the solubility of the solute in the mixture. Although the choices of operating conditions and solvents in re-crystallization are limited, variables such as temperature and solvent compositions can be adjusted and optimized. Knowledge of the solubility behavior of the solute is a prerequisite to understand this important phenomenon, as well as to design and scale-up reliable unit operations for such processes.

The shape of the crystalline solids is also an important factor in downstream processes. Since many solids produced in the pharmaceutical and chemical industries are sold as the end-products, the quality and efficacy of these compounds depend largely on crystal morphology. For example, Mullin (2001) studied the effect of particle shape on the caking of crystals, a condition where the crystalline materials bind together on storage. He found out that small non-uniform elongated crystals are most prone to caking, whereas large uniform granular crystals are the least prone to caking.

The motivation of the present work stems from the earlier work completed by several researchers (Charmolue, 1990; Charmolue and Rousseau, 1991; Gatewood, 1992; Kennedy, 1996). Industrially, L-serine produced from a fermentation process is purified by cooling re-crystallization using methanol as an anti-solvent. It was found by Charmolue (1990) that under certain methanol concentration, the crystals of L-serine changed from needle-shaped, to hexagonal. Analysis from single-crystal diffraction carried out by Gatewood (1992) showed that the hexagonal crystals were L-serine monohydrate, while the needle-shaped crystals were the anhydrous L-serine. Although the effect of methanol on the solubility of L-serine had been demonstrated by Charmolue (1990), the effect of temperature on solubility and the condition at which there is a transition from one pseudo-polymorph to another have not been explored. In the present work, solubility is measured and correlated by varying both methanol concentration and temperature. In addition, the morphology and structure of the solid crystals are studied to gain insights on their solid-state properties. An outline of this research work is presented in Figure 1-1. Cooling re-crystallization experiments were carried out, with the system of study being L-serine in mixtures of water and methanol. The variables in this system

were temperature and solvent composition. At equilibrium, solid crystals were analyzed with an optical microscope, while the liquid samples were taken to determine the solubility using high-performance liquid chromatography. Powder X-ray diffraction method was used to confirm crystal structure and possible pseudo-polymorphic transformation.

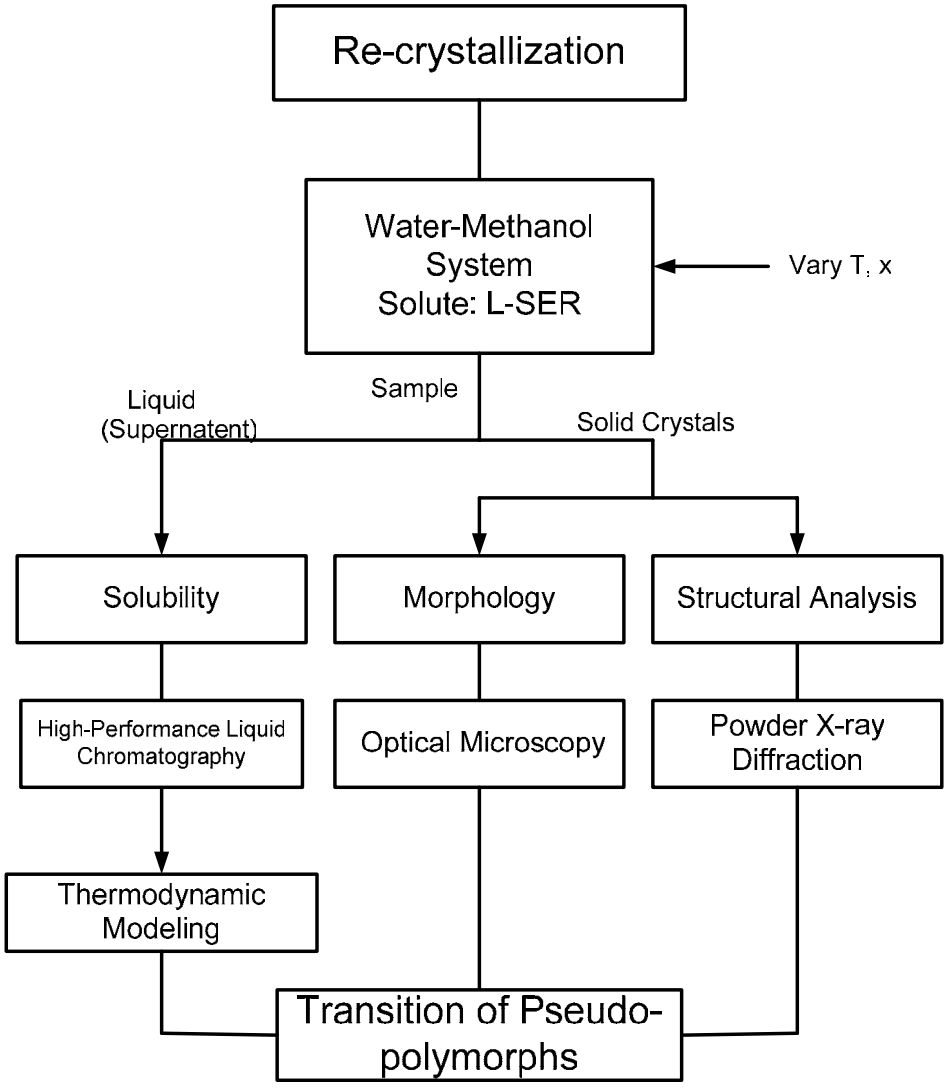

Figure 1-1: Outline of this research project

CHAPTER 2

BACKGROUND

2.1 Properties and Structure of L-Serine

Amino acids are biochemical building blocks. They form short polymer chains called polypeptides or peptides which in turn form proteins. The building blocks of proteins are α-amino acids, which are substances in which the amino group is located on the α carbon atom immediately adjacent to the carboxylic acid group. Approximately twenty α-amino acids are common constituents of proteins. Our bodies can synthesize ten of these in sufficient amount for our needs, while the other ten must be ingested and are called essential amino acids. In humans, the essential amino acids are lysine, leusine, isoleusine, methionine, phenylalanine, threonine, tryptophan, valine, and (in children) histidine, and arginine. All of the amino acids, except glycine, have two optically active isomers designated D- and L-. The D-, or dextrorotatary, form is the isomer that rotates the plane of polarization to the right, while the L-, levorotatary, form rotates the plane of polarization to the left. Although the D, L notation is still applied to carbohydrates and amino acids, it required chemical transformations to establish group relationships, and proved to be ambiguous in its general application. The D, L system is now increasingly replaced with the R, S system adopted by IUPAC, which uses the Cahn-Ingold-Prelog

rules of assigning priority to function group based on atomic number. The L- forms are exclusively present in the living organisms.

L-serine (Figures 2-1 and 2-2) contains 3 carbon atoms with a hydroxyl group (-OH) located at the β carbon. It has a molecular weight of 105.0932 and melting point of 222 ^{o}C, where it decomposes. The common method of preparing L-serine industrially involves fermentation of glycine and methanol by corynebacterium glycinophilum using the enzyme serine hydroxymethyltransferase (Kubota and Yokozeki, 1989).

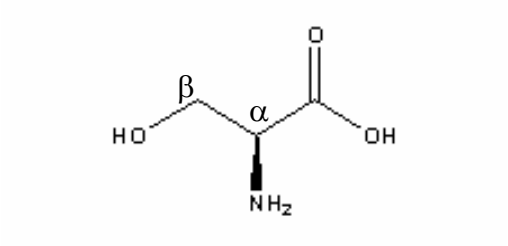

Figure 2-1: Chemical structure of L-serine

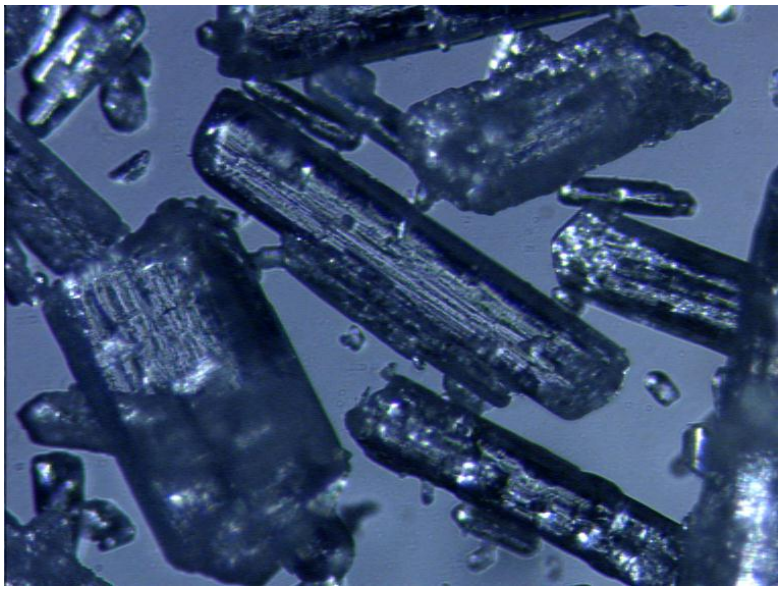

Figure 2-2: Anhydrous L-serine crystals from Ajinomoto, Inc. (5X magnification)

In the crystalline state, the L-serine molecules are in the zwitterionic form with the carboxyl group ($-COO^-$) deprotonated and the amine group containing an additional hydrogen ($-NH_3^+$). Structurally, L-serine has a space group of $P2_12_12_1$ with four molecules per unit cell. A representation of the packing of L-serine molecules in the unit cell is shown in Figure 2-3. Based on the space group, there are three 2_1 screws axes parallel to a, b, and c. By symmetry operation, when L-serine molecule (1) is placed in the position shown in the figure, the position of the L-serine molecule (2) can be determined by translation of the molecule (1) by half a lattice cell length, followed by 180^o rotation around the axis. Similar treatments can be done to obtain the remaining two L-serine molecules in the unit cell.

When water molecules or molecules of D-serine are incorporated into the lattice of L-serine, the arrangement of the hydrogen-bonding changes. This leads to the difference in the conformation of L-serine molecules. This is illustrated in Figure 2-4. A comparison of the unit cell parameters from Table 2-1 shows that this change in conformation causes the unit cell volume to vary. In the case of DL-serine, the crystal system and space group are completely different from that of anhydrous L-serine.

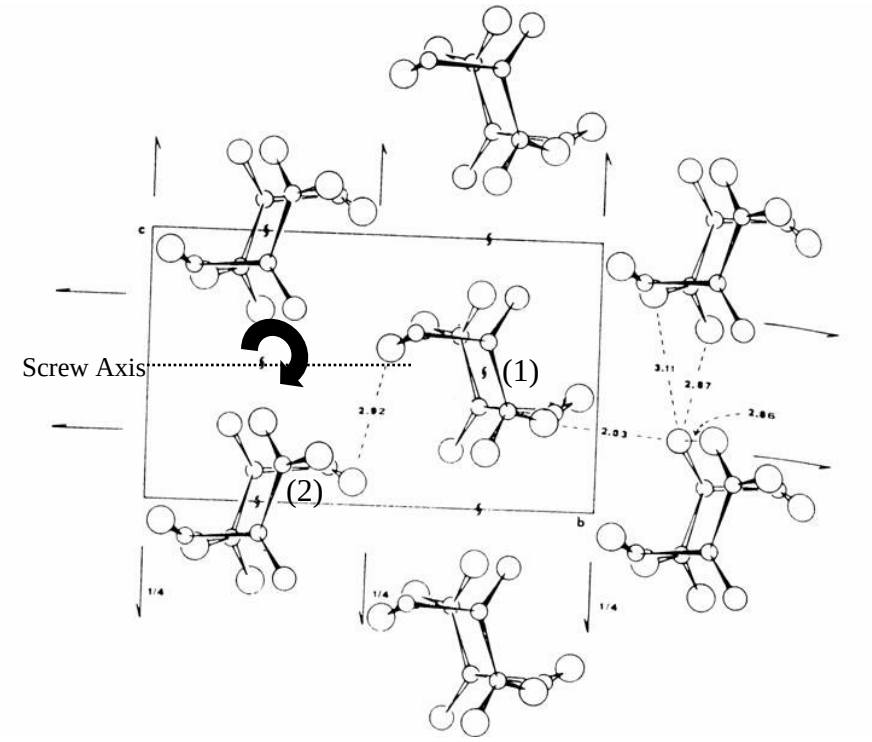

Figure 2-3: Molecular packing of L-serine as view along the a-axis (Benedetti *et al.*, 1973)

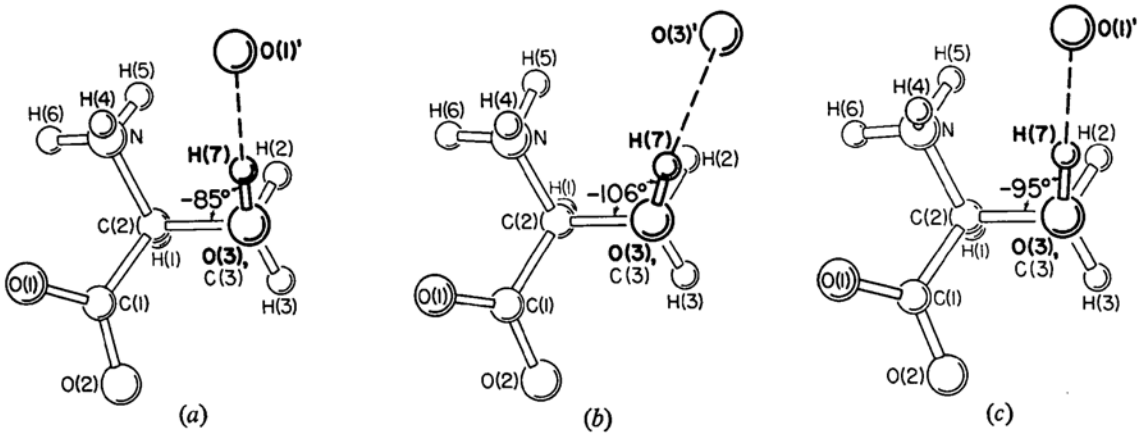

Figure 2-4: L-serine molecules with torsion angles in crystals of (a) DL-serine; (b) anhydrous L-serine; (c) L-serine monohydrate

Table 2-1: Unit cell parameters for anhydrous L-serine, DL-serine, (Kistenmacher *et al.*, 1974), and L-serine monohydrate (Frey *et al.*, 1973)

	Crystal System	Space Group	Z	a (Å)	b(Å)	c (Å)	β
Anhydrous L-Serine	Orthorhombic	$P2_12_12_1$	4	8.599	9.348	5.618	90^o
L-Serine Monohydrate	Orthorhombic	$P2_12_12_1$	4	9.365	12.239	4.835	90^o
DL-Serine	Monoclinic	$P2_1/a$	4	10.739	9.149	4.830	106.42^o

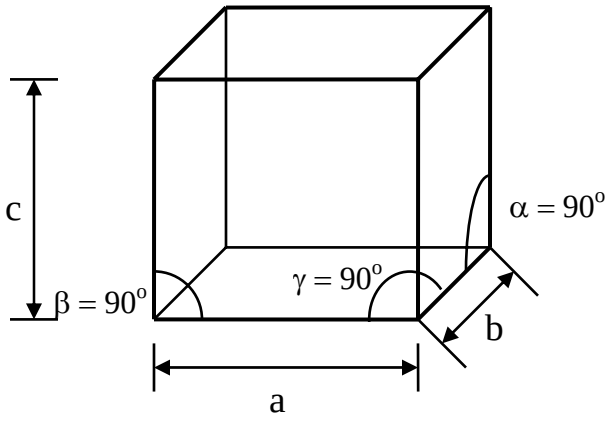

Figure 2-5: Dimensions of the orthorhombic unit cell

2.2

Polymorphism

When two crystals have the same chemical composition but different lattice structure, i.e. different unit cell dimensions and packing, they are called polymorphs (Beckmann, 2000; Brittain, 1999; Giron, 1995; Lefferère *et al.*, 2003; Mullin, 2001). In a sense, polymorphs are different crystalline forms of the same substance in which the molecules have different arrangements and/or different conformations of the molecules. For example, acetaminophen can exist as a monoclinic form, of space group $P2_1/n$ (Haisa *et al.*, 1976), which is thermodynamically stable under ambient conditions. The compound can also be obtained as a less stable orthorhombic form, of space group Pbca, and which has a higher density and hence closer packing (Haisa *et al.*, 1974, and Martino *et al.*, 1996). Compounds that crystallize as polymorphs can show a wide range of different physical and chemical properties depending upon the crystal form. A list of the physical properties that are affected by polymorphism is shown in Table 2-2:

Mullin (2001) provided an important distinction between polymorphs and habit modifications in crystals. Because polymorphs differ in the type of lattice, or in the spacing of the lattice points, they can exhibit different crystalline shapes and may often be readily identified by visual or microscopic observation. These characteristics, however, should not be confused with changes in crystal habits, which are caused solely by changes in the relative rates of growth of specific faces and do not affect the basic physical properties of the substance.

The existence of polymorphism in a product can negatively impact the marketability of that product. For example, the production of Ritonavir, a protease inhibitor for human immunodeficiency virus (HIV) was halt due to the unexpected occurrence of a thermodynamically more stable and less soluble polymorph (Chemburkar *et al.*, 2000). Another example included Glaxo, Inc., who sued Novopharm Ltd. for alleged patent infringement, claiming that Novopharm patented a different polymorphic form of Glaxo's drug, Zantac. Glaxo lost its case and now Novopharm and other generic drug companies sell the new polymorphic form of Zantac (Seddon, 1999).

Table 2-2: List of physical properties that differ among various polymorphs (Grant, 1999)

Packing Properties	Molar volume and density
	Refractive index
	Conductivity, electricity and thermal
	Hygroscopicity
Thermodynamic Properties	Melting and sublimation temperatures
	Internal energy
	Enthalpy
	Free energy and chemical potential
	Heat capacity
	Entropy
	Thermodynamic activity
	Vapor pressure
	Solubility
Spectroscopic Properties	Electronic transitions (i.e. UV absorption spectra)
	Vibrational transitions (i.e. infrared absorption and Raman Spectra)
	Rotational transitions (i.e. microwave absorption)
	Nuclear spin transitions (i.e. NMR spectra)
Kinetic Properties	Dissolution rate
	Rates of solid state reactions
	Stability
Surface Properties	Surface free energy Habit
	Habit
	Interfacial tensions
Mechanical Properties	Hardness
	Tensile strength
	Tableting
	Handling, flow, and blending

2.2.1 Pseudo-polymorphism

Solvent in the surrounding medium may become incorporated into the lattice of crystalline solids in specific stoichiometric ratios. These molecular adducts are termed solvates; when the solvent is water, they are called hydrates. The properties of hydrates and solvates can vary markedly from the primary species (Khankari and Grant, 1995). Pseudo-polymorphism is a term used to distinguish solvates or hydrates from polymorphs.

An example of solvate formation is seen in the phase transformation of taltirelin, a central nervous system activating agent studied by Maruyama and Ooshima (2001). In their study, methanol was used as a co-solvent to promote the transformation of α-form to the β-form. Because of the interaction between the solute and methanol, the pseudo-polymorphs of the β-form were formed ($2H_2O \cdot MeOH$ or $H_2O \cdot 2MeOH$ solvate).

The study of the solubility of meso-1,2,3,4-butanetetracarboxylic acid (BTCA), a formaldehyde-free cross-linking agent for cellulosic textiles, by Morris *et al.* (2004) is an example of hydrates that have different degrees of hydration with time. Experimentally, samples of BTCA were equilibrated with water at 25 ^{o}C for times varying from 1 hour to 36 days. Thermal analysis showed that the products were $BTCA \cdot 2H_2O$ after 1 hour, $BTCA \cdot 4H_2O$ or $BTCA \cdot 2H_2O$ after 5 hours, and $BTCA \cdot H_2O$ after 15 and 36 days.

The pharmaceutical importance of crystalline hydrates has been gaining attention over the last decade, primarily due to the potential impact of hydrates on the development process and dosage form performance (Morris, 1999). Some hydrated compounds may convert to an amorphous form upon dehydration and some may become chemically labile. For example, cephradine dihydrate (Florey, 1973) dehydrates to become

amorphous and undergoes subsequent oxidation. In any case, extra care must be taken in manufacturing and packing such that minimal impact would be done on the regulatory status of the compound.

2.2.2 Monotropic and Enantiotropic Systems

In polymorphism, except at the transition point, only one polymorph is thermodynamically stable under fixed conditions of temperature and pressure. All other forms should be unstable and will eventually transform to the stable form. The more stable form has the lower free energy. For instance, it is first assumed that polymorph II is more stable and therefore has lower free energy than polymorph I. Because of that, the chemical potential of the species in the solid phase II is lower than that in solid phase I, i.e.

$$\mu_{\mathrm{II}} < \mu_{\mathrm{I}} \tag{2.1}$$

Under equilibrium conditions, i.e. for the solid phase in contact with its saturated solution, the chemical potentials are identical for each species in the equilibrated solid and liquid phases, so it is possible to write

$$\mu_0 + RT \ln a_{\mathrm{II}} < \mu_0 + RT \ln a_{\mathrm{I}} \tag{2.2}$$

where μ_0 is the standard chemical potential and *a* is the solution activity. Therefore,

$$a_{\mathrm{II}} < a_{\mathrm{I}} \tag{2.3}$$

and, since activity *a* and concentration *c* are usually related,

$$c_{\mathrm{II}} < c_{\mathrm{I}} \tag{2.4}$$

this leads to the important statement that, at a given temperature, the more stable phase will always have the lower solubility in any given solvent.

If one polymorph is stable under certain temperature range and pressure, i.e. has a lower free energy and solubility, while another polymorph is stable under a different temperature range and pressure, the two polymorphs are said to be enantiotropes, and the system of the two solid phases are said to be enantiotropic. For an enantiotropic system a reversible transformation can be observed at a specific transition temperature. Sometimes a given polymorph is stable at all temperatures below the melting point, and other polymorph is unstable. These polymorphs are said to be monotropes, and the system of the two solid phases is said to be monotropic.

Typical solubility diagrams for species exhibiting monotropic and enantiotropic behavior are shown in Figures 2-6 and 2-7. In Figure 2-6, form II, having the lower solubility, is more stable than form I. These two non-interchangeable polymorphs are monotropic over the temperature range depicted. Examples of this type of system include chloramphenicol palmitate and lamivudine (Grant and Gu, 2001; Jozwiakowski *et al.*, 1996). In Figure 2-7, form II is stable at temperatures above the transition temperature T_{tr} and form I is stable below T. At the transition temperature both forms have the same solubility and reversible transformation between these two enantiotropic forms I and II is possible. Examples showing such behavior include acetazolamide, and metochlopramide (Giron, 1995; Griesser et al., 1997; Mitchell, 1985).

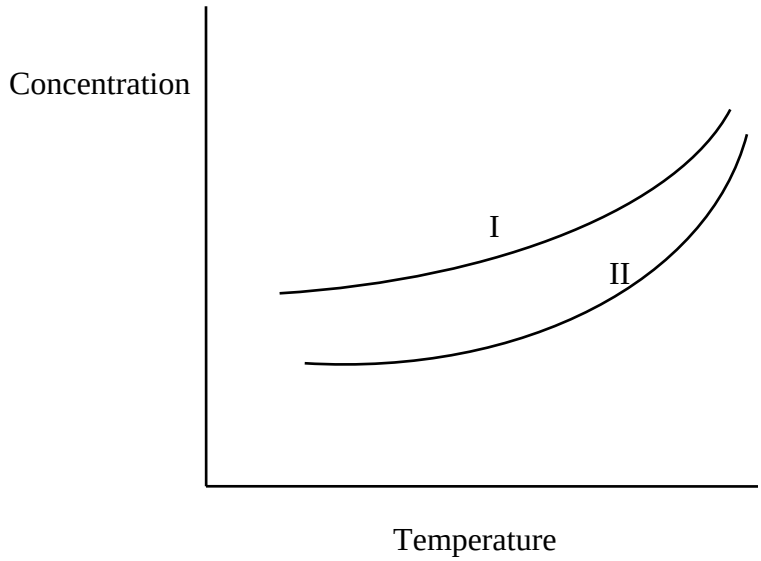

Figure 2-6: Dimorphic monotropic system

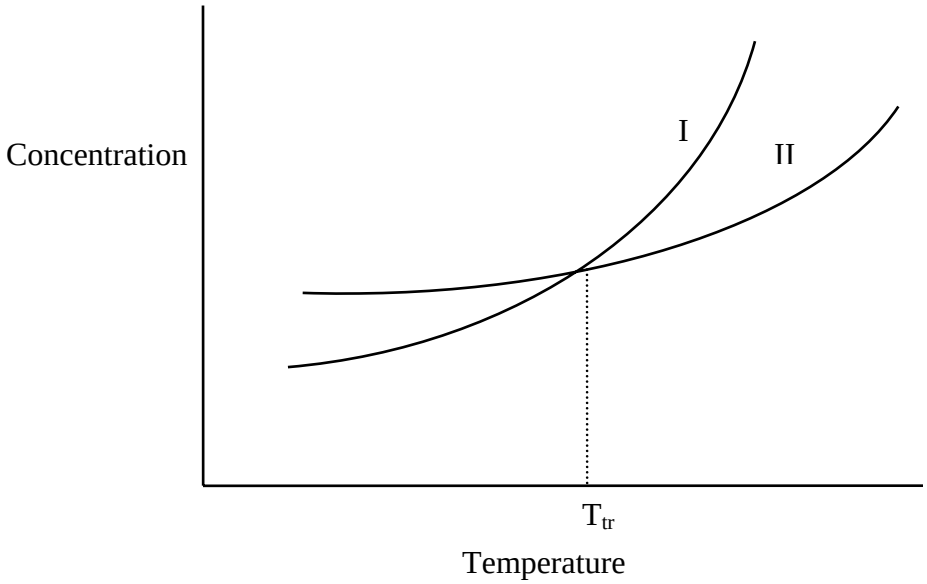

Figure 2-7: Dimorphic enantiotropic system

2.2.3 Transitions of Polymorphs

Interesting yet complex issues were observed by Threlfall (2000) in the transition of polymorphs in the enantiotropic system of dimorphic forms. Several cases were examined using a hypothetical under-saturated solution undergoing cooling crystallization. The solubility and metastable curves of two hypothetical polymorphs, form I and form II, were shown in Figure 2-8. Figure 2-9 illustrates the different zones of crystallization for each polymorph.

(A) When a hot under-saturated solution of initial concentration A is cooled, it will reach saturation and then pass through the metastable zone to a point A1 at which it will spontaneously nucleate and crystallize, and end at point A2 at equilibrium. If the kinetic parameters such as cooling rate are carefully controlled so that the concentration does not cross over the solubility curve of form I, the crystalline product must consist entirely of form II.

(B) If the solution is cooled from point A2, polymorph I has passed the solubility limit, whilst polymorph II has already reached its spontaneous crystallization zone. Hence, the expectation is for polymorph II to be favored. But since polymorph I will always be formed equilibrating below the transition temperature, polymorph I should be favored. This presents a dilemma in which the former is under kinetic control, while the latter case is dominated by thermodynamics.

(C) Cooling a solution of concentration C within area *stuv* will lead to a situation in which the polymorphic outcome is dependent on kinetics, especially on accidental seeding. The solution considered under B will move into this region soon after the onset of crystallization, which may lead to changed driving forces for the formation of each of

the polymorphs. The result is that a mixture of polymorphs, called concomitant polymorphs (Bernstein *et al.*, 1999), is likely to be formed. From this analysis, it is clear that the transition temperature cannot be regarded as a sharp watershed for the determination of polymorph formation. Rather, there is a broad temperature range either side of the transition point within which kinetic effects such as agitation are likely to dominate.

(D) When the solution is cooled from concentration D, the polymorphic form I will always be produced.

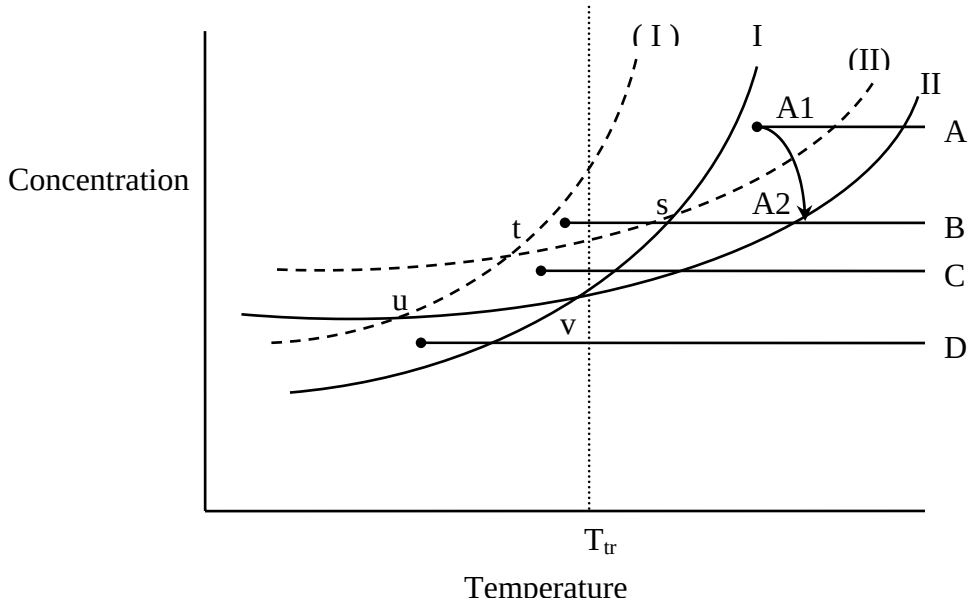

Figure 2-8: Polymorphic system of two enantiomorphically related polymorphs I and II. Solubility curves, solid lines; metastable limits, dashed lines; transition temperature, T_{tr}

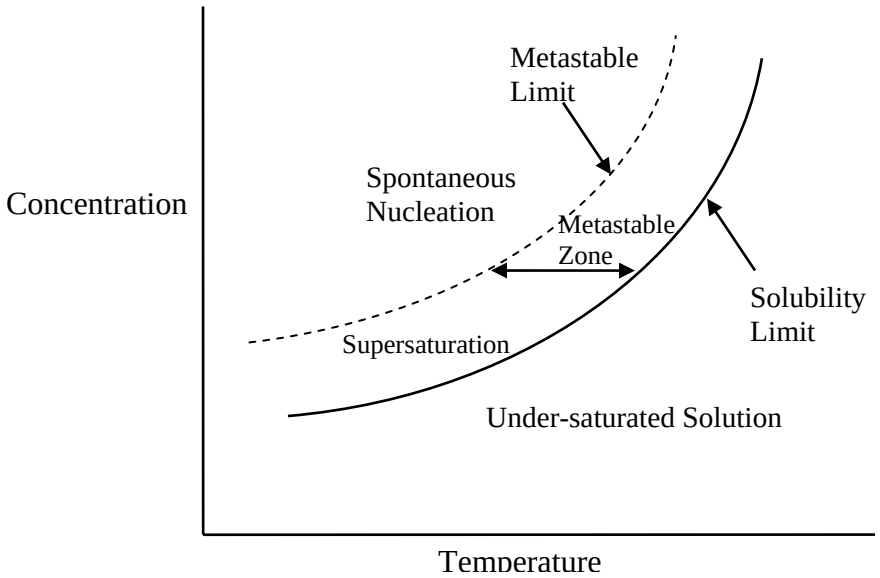

Figure 2-9: Schematic diagram of supersaturation and solubility

2.3

Solubility of Amino Acids

The experimental values of the solubilities of amino acids in water at different temperatures were first measured in the 1930s by Dalton and Schmidt (1933, 1935), and Dunn *et al.* (1933). Some of the solubility data were compiled by Fasman (1976). Solubilities of amino acids in mixed water/alcohol solutions at 25 ^{o}C were reported for water-ethanol (Cohn *et al*., 1934; McMeekin *et al*.., 1935; Nozaki and Tanford, 1971), water-methanol (Charmolue, 1991; Gekko, 1981), water-1-propanol, water-2-propanol (Orella and Kirwan, 1989, 1991), and water-1-butanol (Gude *et al*., 1996a) systems. Few works have taken into account of the influence of the temperature (Dunn and Ross, 1938; Ferreira *et al*., 2004) in water/alcohol mixed solvents.

In the past decade there have been a number of researchers who studied the thermodynamic descriptions and activity models for the solubilities of amino acids in both aqueous and mixed water/alcohol systems. The literature reviewed in this section provides an overview of the different activity models and solubility expressions developed for amino acids in aqueous and mixed-solvent systems, and to emphasize the importance of assumptions and simplifications in parameters reduction.

Nass (1988) adopted a solid-liquid equilibrium treatment based on Prausnitz *et al*. (1999) for amino acids in aqueous systems. The activity and solubility expressions are shown in Eqns. (2.5) and (2.6) respectively.

$$\ln \gamma_i = \ln \gamma_i(\text{Chem}) + \ln \gamma_i(\text{Wilson})$$

$$\text{where } \gamma_2(\text{Chem}) = \frac{x_2'}{x_2},$$

$$\ln \gamma_2(\text{Wilson}) = -\ln\left(x_2 + \Lambda_{21} x_1\right) - x_1\left[\frac{\Lambda_{12}}{x_1 + \Lambda_{12} x_2} - \frac{\Lambda_{21}}{\Lambda_{21} x_1 + x_2}\right],$$

$$\text{and } \Lambda_{ij} = \left(\frac{V_j}{V_i}\right)\exp\left\{-\frac{\left(\lambda_{ij} - \lambda_{ii}\right)}{RT}\right\} \tag{2.5}$$

$$x_i \gamma_i = \left\{\left(\frac{C_p^w - C_p^s}{RT}\right)(T^* - T) - \frac{\Delta H^{\text{sol}}}{RT} - \frac{1}{R}\left[\left(C_p^w - C_p^s\right)\ln\left(\frac{T^*}{T}\right) + \Delta S_{2+4}\right]\right\} \tag{2.6}$$

The activity coefficient γ_i is a summation of the chemical reaction equilibrium term estimated with Henry's law and the physical interaction term estimated with the Wilson equation. The V_j/V_i was set to be the Bondi volumes (Bondi, 1968). The ΔS_{2+4} term was either fixed at zero or used as an adjustable parameter while the C_p^s terms were taken from the literature (Fasman, 1976). Good activity coefficient correlations were obtained for alanine, serine, and threonine. Chen and coworkers (1989) represented the activity coefficients of amino acids using the electrolyte nonrandom two liquid (NRTL) model (Chen *et al.*, 1982). In this model, the long-range interactions were represented by a Pitzer-Debye-Hückel form (Pitzer, 1980) and local interactions were given by a modified form of the NRTL equation. Gupta and Heidemann (1990) proposed the universal functional activity coefficient (UNIFAC) model modified by Larson et al. (1987), to model the activity coefficients of alanine, amino-butyric acid, glycine, hydroxyl-proline, praline, serine, threonine, and valine. Pinho *et al*. (1994) used the original UNIFAC model along with a Debye-Hückel term to account for the activity for the ionic species of amino acids in aqueous solutions. Khoshkbarchi and Vera in 1996 presented a more rigorous technique for correlating amino acid solubility data in aqueous

solution at different temperatures. A simplified perturbed hard-sphere model was developed for the activity coefficients of the amino acids. A modified hard-sphere equation of state was later considered by several researchers (Ghotbi and Vera, 2001; Mortazavi-Manesh et al., 2003).

Regarding the correlations for the solubilities of amino acids in mixed-solvent systems, the works by Orella and Kirwan (1991), and Gude *et al*. (1996a,b) were important contributors to this subject. Orella and Kirwan used an excess solubility approach with the Wilson equation. In order to reduce the number of parameters, a constraint was established based on the fact that the ratio of the activity coefficients of the amino acids was inversely proportional to the relative solubilites:

$$\frac{x_3}{x_3^o} = \frac{\gamma_3^o}{\gamma_3} \tag{2.7}$$

in which x_3^o and γ_3^o are solubility and activity coefficient, respectively of the amino acid in water. The excess solubility of the solute in the mixed solvents was defined using an approach outlined by O'Connell and Prausnitz (1963, 1971):

$$\ln x_3^E \equiv \ln \frac{x_3}{x_3^o} + x_2 \ln \frac{x_3^o}{x_3^{alcohol}} \tag{2.8}$$

The Wilson activity coefficient model is given by the following expression:

$$\ln \gamma_3 = 1 - \ln (\Sigma x_j \Lambda_{3j}) - \Sigma \frac{x_i \Lambda_{i3}}{\Sigma x_j \Lambda_{ij}} \tag{2.9}$$

Λ is the binary solvent-solvent interaction parameter that can be determined by a method that involves minimization of an objective function. Combining Eqns. (2.7), (2.8), and (2.9) yields an equation for correlating the solubility data:

$$\ln x_3^E \equiv \ln\left[x_1 + x_2\left(\frac{\Lambda_{32}}{\Lambda_{31}}\right)\right] - x_2 \ln\frac{\Lambda_{32}}{\Lambda_{31}} + \frac{x_1 x_2 \Lambda_{13}\left(1-\Lambda_{12}\right)}{x_1 + x_2\Lambda_{12}} + \frac{x_1 x_2 \Lambda_{23}\left(1-\Lambda_{21}\right)}{x_1\Lambda_{21} + x_2} \quad (2.10)$$

The initial estimate of the excess solubility can be obtained by assuming $x_3^E \approx 1$. Solubility data of several amino acids in aqueous solutions of methanol, ethanol, 1-propanol, and 2-propanol were correlated to calculate the relative solubilities.

Gude *et al.* (1996a,b) presented a simpler activity coefficient model that included a combinatorial term based on Flory-Huggins theory with a Margules residual expression. The excess solubility expression was simplified based on the fact that the solubilities of amino acids in pure alkanol or mixed water-alkanol solutions were considerably lower than that in pure water.

$$-\ln x_i^E \approx \ln\gamma_i^\infty - \sum_{j=1}^{N}\left(x_j^{'} \ln\gamma_{i,j}^\infty\right) \quad (2.11)$$

Using the following model,

$$\ln\gamma_i = \sum_k x_k \ln\frac{\phi_k}{x_k} + \sum_{j=1}^{N}\sum_{l>j}^{N}\left[A_{jl} x_j x_l\left(1 - C_{jli} x_i\right)\right] + \sum_{j=1}^{N} A_{ji} x_j x_i \quad (2.12)$$

$i = solute;\ j,l = solvents;\ k = both$

where A_{jl} and A_{ji} were solvent-solvent and solvent-solute interaction parameters respectively, $\phi_k = x_k r_k / r$ with $r = \Sigma_k x_k r_k$. These were all estimated with appropriate methods. C_{jli} represents the ternary interaction parameter. The final excess solubility expression for correlation is the following:

$$\ln x_i^E = \ln r' - \sum_{j=1}^{N} x_j^{'} \ln r_j + r_i\left(\frac{1}{r^{'}} - \sum_{j=1}^{N}\frac{x_j^{'}}{r_j}\right) + \sum_{j=1}^{N}\sum_{l>j}^{N}\left[A_{jl} x_j^{'} x_l^{'}\left(1 + C_{jli}\right)\right] \quad (2.13)$$

Solubilities for serine, glycine, alanine, tyrosine, isoleucine, phenylalanine, and tryptophan in mixture of aqueous 1-butanol solutions were correlated by adjusting only the ternary interaction parameter, C_{jli}.

The above discussions presented some approaches in correlating the solubility data and the appropriate activity coefficient models for amino acids in different solvent systems. In general, when system moves from binary (amino acid + water) to ternary (amino acid + water + alcohol), the interactions between the solute and solvent molecules, as well as the different solvent molecules themselves, become more complex. Researchers in this field are often faced with tradeoffs between parameter reduction and model accuracy. In Chapter 4, a simple solubility model using the principle of thermodynamic cycle is derived. This model is used to correlate the solubility data of L-serine in mixed water-methanol solution, and to determine the transition temperatures and dissolution parameters.

CHAPTER 3

EXPERIMENTAL METHODS

3.1 Solubility Measurement

3.1.1. Equilibrium Cell

The experimental setup for solubility experiments is shown in Figure 3-1. A 3-port, 150-mL jacketed crystallization vessel was used as the equilibrium cell. The jacket of the vessel was connected to a water circulator system with programmable temperature-control. Constant mixing was provided by a magnetic stir bar. Sampling apparatus is shown in Figure 3-2. Liquid samples were withdrawn from the equilibrium cell using a 5-mL plastic syringe and a 15 PS stainless steel needle. A 0.20-μm syringe filter was used to prevent fine solid crystals from entering into the syringe. Table 3-1 lists all equipment used in the solubility experiments.

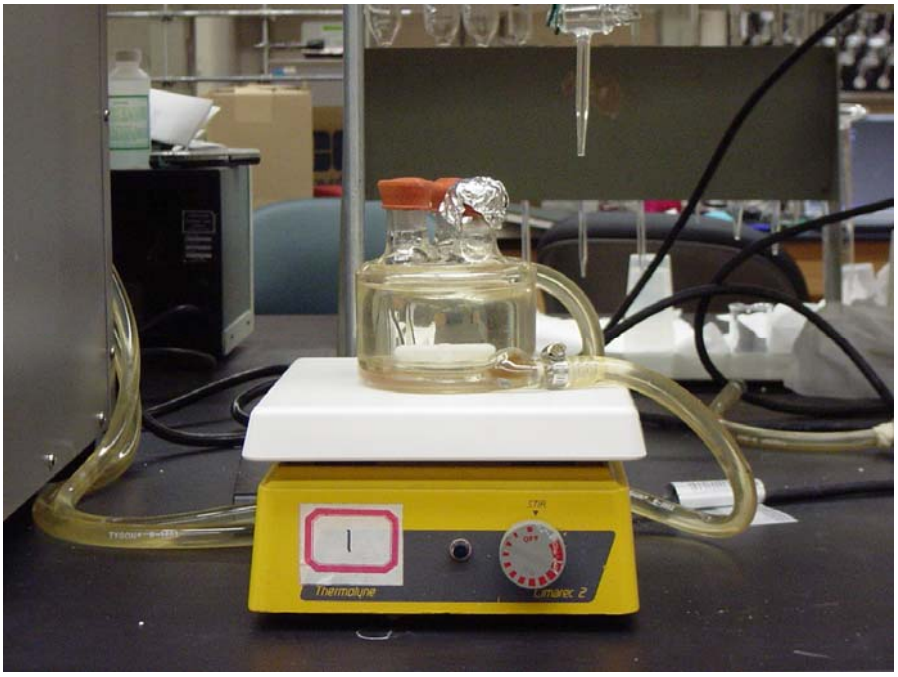

Figure 3-1: Two 3-port, 150-mL jacketed crystallization vessel with attached tubing and rubber stoppers

Figure 3-2: The 5-mL single-use plastic syringe, 0.20 μm syringe filter, and 15 PS needle for sampling

Table 3-1: Apparatus used in the solubility experiments

Item	Description	Vendor/Manufacturer	Catalog Number
Analytical Balance	Capacity 210g x 0.1mg	Ohaus	Model AP250D
Buret	Kimax® 50-mL manual titrator	Various	
Cap, HPLC Vial	Cap and septa, yellow	Sun International	500065
Circulating Baths	Model 1157 & 1157P, 13L programmable heated/refrigerated circulators	VWR International	13270-540; 13271-106
Equilibrium Vessels	150-mL jacketed glass vessels with 3 addition ports	GT Chemistry Glass Shop	Custom made
Laboratory Oven	Isotemp® 500 Series	Fisher Scientific	13-246-526G
Magnetic Stir Bars	Teflon coated 1 1/2" in length	Various	
Magnetic Stir Plates	Model No S46725 ceramic top magnetic stirrers	Fisher Scientific	11-496-31
Needle	4" 15PS Type 304 stainless steel	VWR International	20068-783
pH meter	pH340 pH meter with Sentix 41-1 electrode	WTW measurement systems, Inc.	
Pipet Aid	4W pump pipeter	Drummond Scientific Co.	
Pipet Tips	1250 μL, 100 μL	VWR International	53508-918, 53512-330
Plastic Syringe	5 c.c. single-use syringe	Fisher Scientific	14-817-29
Rubber Stopper	Size S15 laboratory stoppers	Various	
Syringe Filter	0.20 μm Surfactant free cellulose acetate	VWR International	28200-016
Solvent Bottle	1L Pyrex® brand media bottle	Fisher Scientific	06-414-1D
Stop Watch	1/100 second recording	Various	
Thermocouple for Oven	Grounded 6" type T 1/16" diameter	Omega Engineering, Inc.	
Thermocouple Thermometer	6" Type K	Barnant Company	Model 600-1040
Tubing	Tygon® 3/8"x1/2"x1/16" flexible tubing	ES&T Stockroom	0365
Vial, HPLC	12 x 32mm class glass vials	Sun International	200250
Vortexer	Vortex-Genie 2 un-timed 60Hz	VWR International	58815-234

3.1.2 Experimental Procedures

Care was taken to clean all equipment thoroughly to prevent solubility enhancement or reduction due to impurities. One 150-mL jacketed vessel, three rubber stoppers, and one magnetic stir bar were washed with soap and rinsed with tap water. They were then rinsed with deionized water three times and placed in the laboratory oven with the stirrer bar inserted inside the vessel. Once completely dry, the three rubber stoppers were placed in the ports over the vessel containing the magnetic stirrer. One of the rubber stoppers was pierced to allow the insertion of sampling needle. It was then wrapped with aluminum foil to prevent exposure to impurities. Tygon® tubings were connected from the inlet and outlet ports of the equilibrium cell to a water circulator and the desired temperature was set.

At this point, a fixed amount of water was added to the vessel and the system was agitated to create a vortex and pre-heated to 60 ^{o}C. L-Serine was added into the solution manually through the addition port until no further L-Serine could be dissolved. The temperature of the solution was held constant for 10 to 15 minutes and then raised to 10 ^{o}C above the desired temperature. If the solution became clear, an additional small quantity of L-serine was added; this was repeated until only a slight amount of crystalline L-serine was present in the solution. An unsaturated solution was achieved by another 5^{o}C increase in the temperature. The conditions were held constant for about 30 minutes to ensure that no crystals were present in the solution.

After the 30-minute interval, visual inspection was performed to check for evidence of crystallization in the vessel. If crystals formed, the experiment was terminated and a new batch of solution had to be prepared. In most cases, however, clear

solutions were observed and they were maintained at the temperature for about 30 minutes. After that, the temperature set point of the circulator bath was changed to 60 ^{o}C.

Prior to addition, around 50-mL of methanol was prepared in a glass bottle and pre-heated. Once the desired temperature was reached, a buret was used to dispense a fixed amount of methanol slowly into the vessel. The system was kept sealed after the addition. Volumes of water and methanol were added in amounts that brought the approximate final volume to 100 mL. Usually, nucleation occurred after methanol addition. The system was allowed to equilibrate, which, according to Charmolue (1990), should occur after 4 hours. This was taken as the minimum time for sampling. The volumes of water and methanol can be converted to mass-unit using the densities at the temperatures at which volumes were measured. Density of water were obtained from Table 2-28 on Perry's Chemical Engineer's Handbook (1999); while density of methanol at 60 ^{o}C was determined experimentally, as described in Appendix A. The percentage of methanol in the solution was then converted mole-unit from knowledge of the molecular weights of methanol and water.

3.1.3 Sampling Protocol

A series of samples were taken from the equilibrium cell over the temperature range of 0 to 60 ^{o}C. If no crystals appeared within a short period of time at the desired temperature, the set point was lowered by 5 ^{o}C intervals until crystals formed. After crystals were observed in the solution, the system conditions were held constant for around 8 hours. When the system reached equilibrium at the desired temperature, samples were taken from the solution using the following techniques. First, a 0.20-μm sterile syringe filter was secured to the Luer-lock end of a 5-mL single-use plastic syringe, and a 15 PS needle was attached to the filter. They were then pre-heated or pre-cooled in the laboratory oven or refrigerator to the desired temperature. During sampling, the temperature of the solution was measured using a Type-T thermocouple. The aluminum foil covering the rubber stopper was temporally removed and about 1-mL of the solution was filtered and collected into the syringe. If the collected solution contained crystals, sample was discarded and new sample taken. At this time, the syringe filter and needle were detached and a few drops of the solution were injected into a 12 x 32 mm vial containing HPC-grade water for immediate dilution and weighed. The contents of the vial were then mixed by a vortexer. The sampling needle was then cleaned with at least 30 mL of HPLC-grade water and dried in laboratory oven before next use.

A schematic diagram of a typical sampling protocol is shown in Figure 3-3. Solution is cooled and samples were taken at temperatures in the order of 60^{o}C, 50^{o}C, 40^{o}C, 30^{o}C, 20^{o}C, and 10^{o}C. Cooling is controlled at the rate of 10^{o}C/hr. Addition samples might be taken in between those temperatures depending on the number of data needed. To minimize re-dissolution of the crystals, no re-heating was performed.

Several treatments were done to ensure accurate sampling of the liquid supernatant. The 15 gauge needle had a fine inner diameter (~1.7mm) and this served to exclude the larger crystals. Furthermore, the 0.20 μm syringe filter was attached when sample was withdrawn from the solution. Any crystal that may have drawn through the needle would be retained by the filter. In addition, the needle, syringe filter and syringe were pre-heated/pre-cooled prior to sampling to prevent crystallization of L-Serine from occurring in the needle, filter, or syringe.

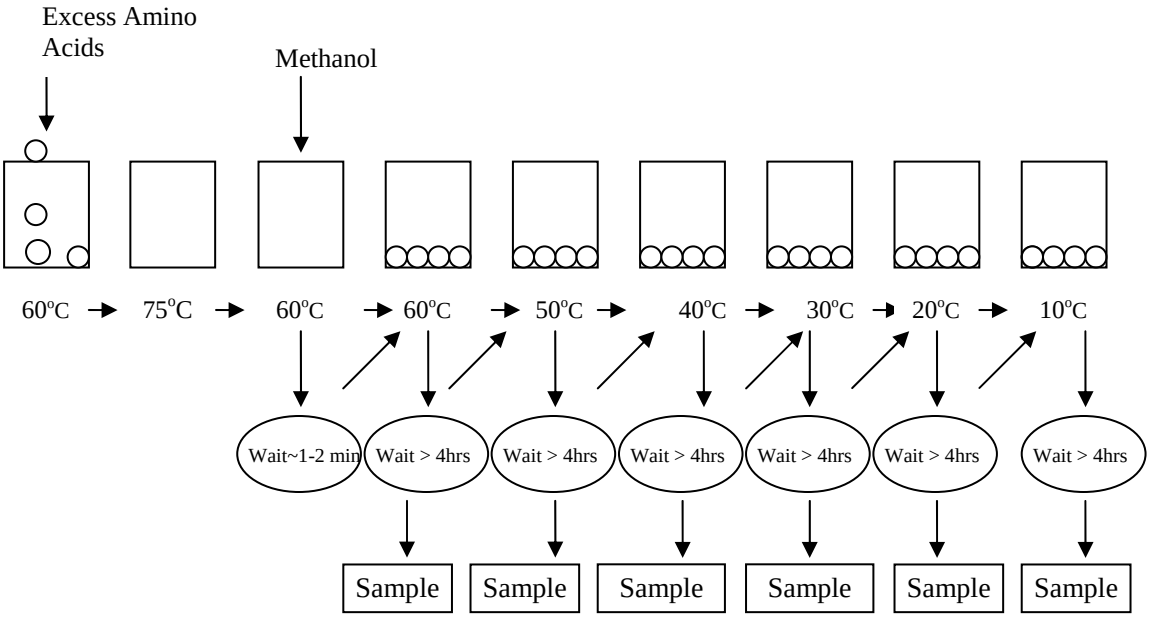

Figure 3-3: Typical sampling protocol for the solubility experiments

3.1.4 High Performance Liquid Chromatography

3.1.4.1 Equipment

The use of high performance liquid chromatography (HPLC) in determination of amino acids has gained popularity for the past 2 decades (Hill *et al*, 1979). In this study, HPLC was used to measure the concentrations of L-serine at equilibrium. Two high-performance liquid chromatography systems from Shimadzu® were employed for measurement of L-Serine concentrations at equilibrium. They are shown in Figure 3-4. The 10A-VP series consists of a SCL-10Avp system controller, a LC-10ATvp solvent delivery unit, a SIL-10Avp auto injector, a SPD-10AVvp UV-VIS spectrophotometric detector, a DGU-14A on-line degasser, and a FCV-10ALvp gradient flow control value. The 10A series is equipped with a SCL-10Avp system controller, two LC-10AS solvent delivery units (A & B), a SIL-10A auto injector, and a SPD-10AV UV-VIS spectrophotometric detector. Degassing of mobile phases is done by a DGU-14A on-line degasser for the 10A-VP series. A Helium sparging method is employed for the 10A series where the solvents are purged with Helium (Ultra high purity, size 300, catalog # UHP300, Airgas South, Inc.) for 10 minutes prior to use. Both systems used a reversed-phase packed column (Microsorb-MV, 100-5 C_{18} 150 x 4.6 mm, Catalog # R0086200D5, Varian) for separation of amino acids. The absorbance of energy by the amino acids was detected by the UV-Visible detector and was translated as voltage during the time program. These data were acquired using CLASS-VP Chromatography Data System version 7.2.1 software program operated on a personal computer.

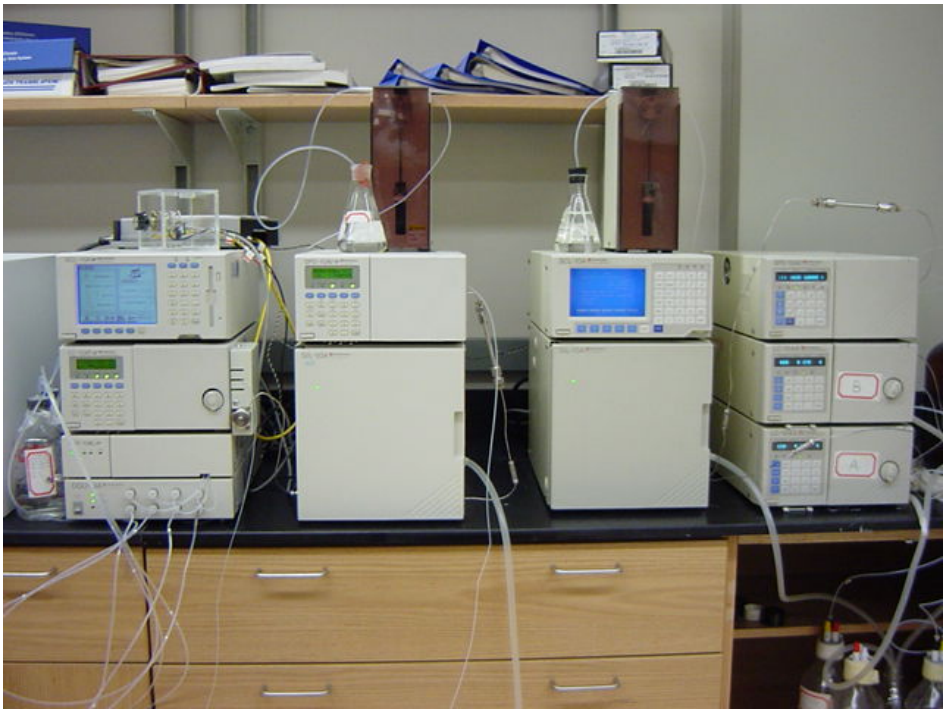

Figure 3-4: The high-performance liquid chromatography systems

3.1.4.2 Analytical Schemes and Amino Acids

The amino acid analytical scheme developed by Charmolue (1990) was employed with slight modifications to the mobile phases and solvent elution protocol. L-aspartic acid (tissue culture grade, catalog # FLBP374-100, Fisher Scientific) was chosen as the internal standard since it has shorter retention time than L-serine which enabled a short analysis time (~15 minutes). L-serine was procured from Ajinomoto U.S.A., Inc. and was used without further purification. A linear gradient elution method with two mobile phases was used to effectively separate the amino acids. This method allowed the composition of the solvents with different polarity to change with time, so the compounds of interest would elude out separately with distinct retention times.

3.1.4.3 Preparation of Mobile Phases

Solvent A was a methanol-based solution that consisted of 65 vol% methanol (Methanol Optima*, catalog # A454-4, Fisher Scientific) and 35 vol% water (HPLC-grade, Catalog # W5SK-4, Fisher Scientific). Solvent B was a water-based solution. The procedure to make 1L of solvent B is the following: 0.05 mol (~7.1 g) of anhydrous sodium phosphate dibasic (ULTRAPURE BIOREAGENT, 99.0% min, catalog # JT4062-1, VWR International) were added to 960 mL of HPLC-grade water in the glass solvent bottle and mixed. After all sodium phosphate had been completely dissolved, 0.05 mol (~6.8 g) of sodium acetate trihydrate (catalog # S220-1, Fisher Scientific) was added to the solution and mixed. Then 20-mL of tetrahydrofuran (HPLC-grade, 99.9%, catalog # AC610100040, Fisher Scientific) and 20-mL of methanol were added, the pH of the solvent was reduced to 7.2 by dropwise addition of concentrated hydrochloric acid

(1.000 N, catalog # VW3202-1, VWR International) to prevent damage to the column. Both solvents were stored in the refrigerator before use.

3.1.4.4 Time Program and Acquisition Parameters

The absorption wavelength was determined by performing a spectrum scan 254 – 370 nm with scan step of 2 nm on the Deuterium lamp. Maximum absorption was observed around 330 – 340 nm. The wavelength of 334 nm was chosen for all analyses. The linear gradient time program, pump settings, and acquisition parameters are presented below. The total flow rate was fixed at 1 mL/min. The percentage of solvent A increased linearly from 0 % to 100 % during the first ten minutes, causing the polarity of mobile phase to decrease. This allowed the less polar L-aspartic acid to elude out at around 7.6 minute. From 10 to 15 minutes, the flow rate of solvent B was 0 while the flows rate of solvent A remained constant at 1 mL/min. L-serine eluded out during this period at around 12 minute. After that, the percentage of solvent B slowly increased back to 100 % and equilibrated for the next run. A typical chromatogram is shown in Figure 3-6.

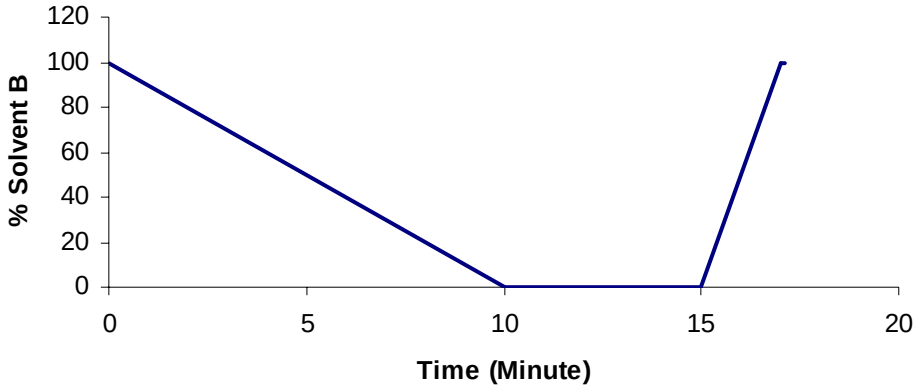

Figure 3-5: Solvent gradient elution scheme with reference to solvent B

Time (min)	% Solvent B
0.01	100
10.01	0.0
15.01	0.0
17.01	100

Total Flow Rate: 1 mL/min

Initial Solvent B Concentration: 100%

Pressure limits: 0.0 – 35.0 MPa

Lamp for Detector: Deuterium (D2)

Wavelength for Acquisition Channel: 334 nm

Sampling Frequency: 2 Hz

Acquisition Time/Controller Stop time: 17.11 min

Injection Volume: 5 μL

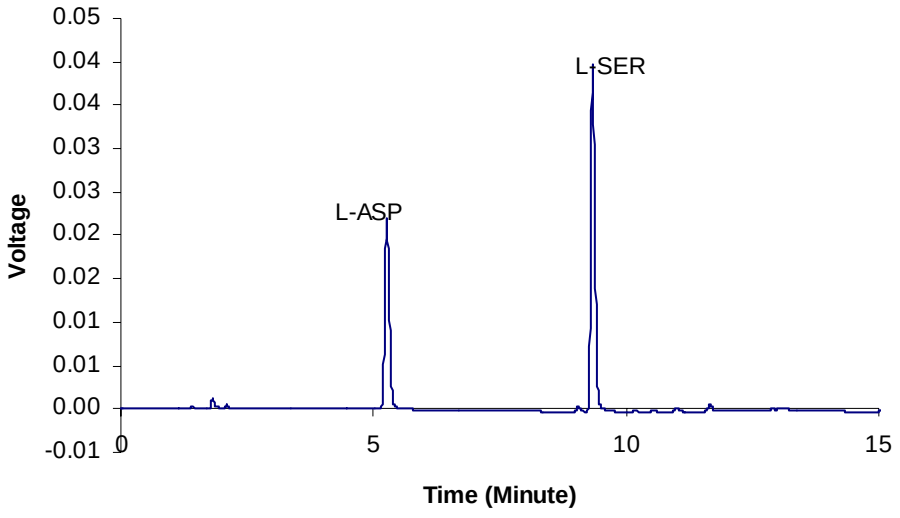

Figure 3-6: HPLC separation of L-aspartic acid and L-serine

3.1.4.5 Calibrations

The peak area calculated by integration of peak intensity in a component of a sample is generally proportional to its concentration. However, this is not always the case since the HPLC conditions such as the efficiency of the column, amount injected, and sensitivity of detector, are not exactly the same for every run. For this research, an internal standard method was used. In this method, the ratio of the sample peak area to standard peak area is proportional to the ratio of the sample concentration to standard concentration. The relationship can be represented by the following equation:

$$\frac{A_S}{A_I} = k\frac{C_S}{C_I} + b \tag{3.1}$$

From this equation, *A*, *C* are peak area, and concentration in g/g solution respectively. *k*, *b* are the constants for this linear equation. The subscripts *S* and *I* denote sample and internal standard respectively. By preparing solutions of known concentrations of L-serine and L-aspartic acid and recording their corresponding peak areas, *k* and *b* can be determined. The calibration procedure is shown in Figure 3-7. Experimentally, standard solution of L-serine (~1 g /100 g water) and L-aspartic acid (~ 0.5 g / 500 g water) are prepared. For the case of L-aspartic acid, mild stirring with magnetic stirrer might be required to dissolve all solids. Both standard solutions were kept in the refrigerator prior to use. Five to six samples were prepared by adding 0.01 – 0.08 g of L-serine, 0.2 g of L-aspartic acid into water to make up 1 g of solution. The concentrations of the L-serine and internal standard after the first dilution were determined by the following Eqns. (3.2) and (3.3):

$$C_{S2} = C_{S1} \times \frac{M_{S1}}{M_{S1} + M_{I0} + M_{W1}} \tag{3.2}$$

$$C_{I1} = C_{I0} \times \frac{M_{I0}}{M_{S1} + M_{I0} + M_{W1}} \tag{3.3}$$

About 0.1 g of this solution was then diluted with 0.9 g of OPA in a HPLC vial and injected into the column for separation. The final concentrations and the equation for linear regression are the following:

$$C_{S3} = C_{S2} \times \frac{M_{S2}}{M_{S2} + M_{OPA}} \tag{3.4}$$

$$C_{I2} = C_{I1} \times \frac{M_{I1}}{M_{I1} + M_{OPA}} \tag{3.5}$$

$$\frac{A_S}{A_I} = k \frac{C_{S2}}{C_{I1}} + b \tag{3.6}$$

Since A_S and A_I can be obtained from the chromatogram, one can fit values of A_S/A_I versus C_{S2}/C_{I1} to determine the equation of the calibration curve. Re-calibrations were performed routinely since the separation efficiency declined with use. All calibration curves used in the experiments are included in Appendix B.

3.1.4.6 Sample Dilution and Derivatization

Dilution of sample is necessary to prevent crystallization of the dissolved L-serine, which reduces the accuracy of HPLC analysis. Furthermore, UV detection is most sensitive and accurate for low amino acid concentrations (~10^{-5} g amino acid/g solution). Therefore, dilution of sample and internal standard are required to allow the concentrations to reach optimal detectable range. Figure 3-7 depicts the dilution scheme for the experiment. Subscripts S, W, and I stand for sample, water, and internal standard respectively. M is the weight of solution in gram and C is the concentration in g solute/g solution.

During sampling, about 1-mL of solution was withdrawn from the vessel, two drops (M_{SO}, ~0.5 – 0.9g) were added into the vial containing about 1.5 – 1.7g (M_{W0}) of HPLC-grade water. The contents were then mixed by a vortexer immediately. A second vial was placed on the analytical balance and tared. A predetermined amount of the sample (M_{S1}) was added to M_{I0} of the internal standard and M_{W1} of water. M_{S2} of the resulting mixture was diluted M_{OPA} of o-phthalaldehyde (OPA) for pre-column derivatization (Roth, 1971) and the stop watch was started. Exactly after 5 minutes, the auto injection sequence of HPLC was initiated. From Eqn (3.6), since we know k, b, A_S, and A_I, C_{S2} can be determined. C_{S0} can then be obtained by back calculation.

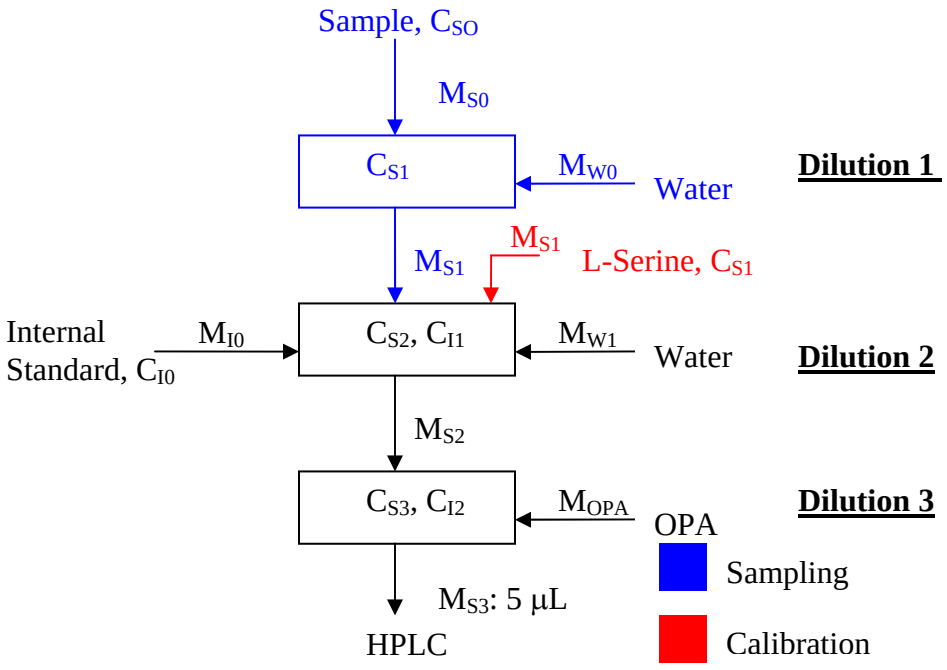

Figure 3-7: Dilution scheme for detection in HPLC

3.2

Structural Analysis of Crystals

3.2.1 Optical Microscopy

Change in the size and shape of the crystals are often encountered during re-crystallization. Kinetic factors such as agitation and cooling rate would alter the size of the re-crystallized solids. Also, the crystals may change from one morphology to another which may indicate a phase transition. Optical microscope was therefore employed to study the effect of solvents on the morphology of L-serine.

Small quantities of L-serine crystals were collected from the solution mixture and analyzed with the optical microscope prior to each sampling. This is to ensure that the system has reached its equilibrium, i.e. at equilibrium, only one stable form should be present. The crystals were collected with a single-use polyethylene pipet and placed on glass slides. Usually, paraffin oil was added to slow down evaporation of solvents. The slides were then placed on the stage of Meiji optical microscope, which had a 10x eyepiece and 3 objective lenses for magnifications of 2.5x, 4x, and 10x. The Image-Pro Plus software version 4.5.1.29 was used to provide live-preview of the crystals and the microscopic images were taken with a Sony digital photo camera (Model DKC-5000, 0.6 x). Refinement of the images such as image scale, crystal size measurements was done using the software.

3.2.2 Powder X-Ray Diffraction (XRD)

Optical microscopy only provides information on the external shape or habit of the crystals. Several methods for structural determination of solid-state structures have been developed. They include spectroscopic techniques such as nuclear magnetic

resonance (NMR), infrared, UV-visible, Raman, mass, optical spectroscopy, and physical techniques such as calorimetry, neutron and electron diffraction, and X-ray crystallography. The X-ray crystallography method was used in structure analysis of L-serine crystals. There are two types of X-ray diffractometry (XRD): single-crystal XRD and powder XRD. The single-crystal XRD can generate structure data in three-dimensions but require larger single crystals (>100 μm), while the powder XRD use smaller crystals but only provide data in one-dimension. Prior work on L-serine crystals was done using single-crystal XRD with success (Gatewood, 1992). There was, however, no accessible single-crystal XRD at present. The powder XRD method was used in the course of this study.

3.2.2.1 Crystal Sample Preparation

It was observed that the L-serine monohydrate crystals tended to lose their crystalline properties and dehydrate during the drying process (Gatewood, 1992; Frey *et al*, 1973). Hence care must be taken to ensure no moisture other than that on the surface of the crystal lattice was removed. At the end of each set of solubility experiments, the morphology of the crystals was first confirmed with an optical microscope. The solution from the equilibrium cell was then filtered under vacuum using a 0.2-μm filter paper (Membrane filter, MCE, 47mm, catalog # 09-719-2B, Fisher Scientific). The filtered crystals were immediately stored in a 50-mL beaker sealed with parafilm to prevent water loss. No further drying should be done.

3.2.2.2 Apparatus and Procedures

A Scintag XDS-2000 Advanced Diffraction System located in room 2-54 of Boggs Chemistry building was used to collect intensity data for the L-serine anhydrate

and monohydrate crystals. The system was equipped with Cu Kα radiation source with wavelength of 1.540562 Å. A Scintag program DMSNT version 1.37 was used to convert signal from the detector to intensity pattern and to perform search-match procedure with the ICDD (International Centre for Diffraction Data) database. The crystal samples were first ground with a mortar and pestle to powder form (~10 μm). They were then packed into a standard aluminum sample-holder and placed onto the spring loader of the diffractometer. The settings for the diffractometer are summarized in Table 3-2. A preliminary analysis was done and it was found that the intensity of the largest peak was too high (> 30,000 CPS), suggesting that there were preferred orientations of the crystals on the sample holder. Preferred orientation occurs when the powder sample produces a uniform cone of diffracted radiation for each *hkl* plane that results in a uniform intensity measurement (Byrn *et al*, 1999). For example, if several plastic straws are thrown into a shoe box, the straws will most likely align parallel to each other. Needle-like or plate-like crystals are more prone to preferred orientation, as it is the case for the L-serine crystals. To resolve this issue, a side-loading aluminum sample-holder was used to ensure the powder crystals were packed randomly. Figure 3-8 shows the pattern of the anhydrous L-serine from the manufacturer. The side-loading technique was found to be effective in eliminating the preferred orientation and peak-slitting (occur at intensity >30,000 CPS). All remaining samples were analyzed using the side-loading sample-holder.

Table 3-2: Settings for powder XRD measurements

Parameter	Value
Scan Angle	10 – 50 ^{o}
Scan Mode	Continuous
Step Size	0.02 ^{o}
Scan Rate	1.2 ^{o}/min
Current	40.0 mA
Voltage	-45.0 kV
Filament Current	~ 3.22 A
Maximum Tube Power	~ 1.80 kW

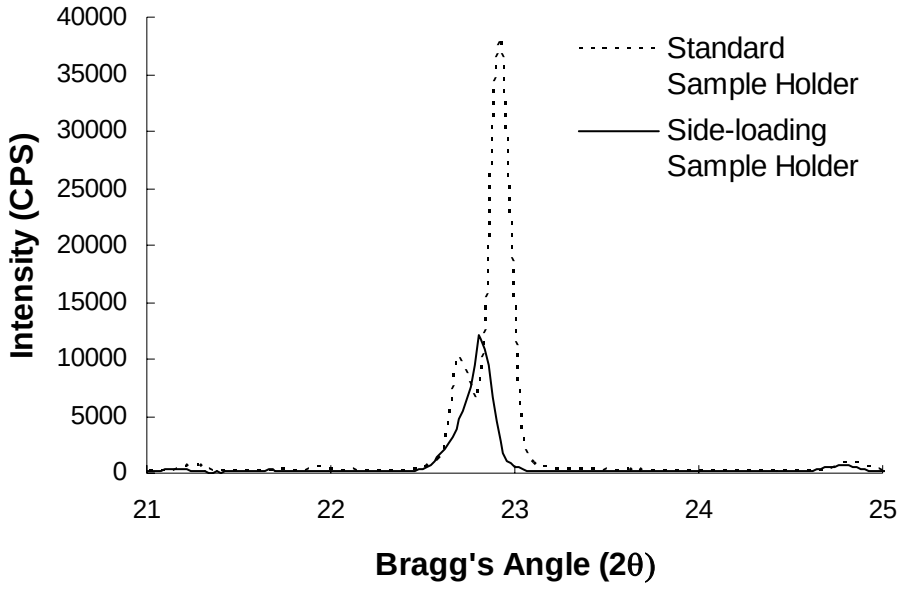

Figure 3-8: Comparison of the intensity pattern of the standard sample holder to that of the side-loading sample holder

3.2.2.3 Comparison of Powder Patterns

The intensity patterns from the Scintag XRD were compared with the crystallographic data from the ICDD database and the calculated pattern from Cerius^2.

A PCPDFWIN software was used to retrieve and display records from the ICDD database. Only file data of the anhydrous L-serine (card # 27-1989) and DL-serine (card # 22-1931) were found. This software was provided on the computer dedicated to the Scintag XRD. In the data file, the Bragg's angles where there is diffraction, the corresponding intensities, and the *hkl* plane were recorded.

Since intensity pattern for L-serine monohydrate was not available from the ICDD database, a set of powder pattern was calculated using the program Cerius^2, version 4.2. This program was developed by Accelrys, Inc. First, the single-crystal X-ray data, i.e. space group, unit cell parameters, fractional co-ordinates of the atoms, and temperature factors, was used to define the spatial co-ordinates for the atoms of the L-serine molecules in the unit cell. Second, a graphical molecular model was simulated with the crystal builder module. This simulated molecular model can be viewed using the Materials Visualizer, a function of MS Modeling, version 3.0.1, developed by Accelrys, Inc. Then the analytical module was used to calculate the powder pattern by inputting the parameters such as radiation source and wavelength.

The powder patterns from measurements and those collected from the ICDD database and the calculated pattern were compared and overlayed to gain insight on the structure of the crystal samples.

CHAPTER 4

RESULTS AND DISCUSSIONS

4.1 Solubility of L-Serine in Mixtures of Water and Methanol

4.1.1 Data in the literature

4.1.1.1 Solubility

Although a very simple yet important biochemical molecule, there has been a limited number of published solubility data for L-serine. Hade measured the solubility of L-serine in pure water for the temperature range of 0 – 40 ^{o}C in 1962 and his data were reported by Hutchens in the *Handbook of Biochemistry and Molecular Biology* (Fasman, 1976). Only five values at different temperatures were given. With the advance in amino acids purification and analytical chemistry, Charmolue in 1991 updated the database for the solubility of L-serine in pure water with more values and an extension of the temperature range of such data to 50 ^{o}C. Dey and Lahiri (1986) determined the solubility of L-serine in methanol-water, ethanol-water, and 2-propanol-water at 298 K (1986). In his work, Charmolue reported the solubility of L-serine in methanol-water solutions at 283 K and 303 K (1991). Only one literature source took into account the effect of temperature on the solubility of L-serine in methanol-water solutions (Dey and Lahiri, 1988), but these data merely covered a narrow range at the low temperatures

(288 K, 293 K, and 298 K).

4.1.1.2 Anhydrous and Monohydrate Formation

The hydration of amino acids has been widely reported (Goto and Isemura, 1964; Sidorova *et al*., 1971; Pominov *et al*., 1972; Gusev *et al*., 1974; Fasman, 1976; Hollenberg and Ifft, 1982; Kotova *et al*., 2002) and investigated (Greenberg *et al*., 1978; Carozzo *et al*., 1978; Goodfellow *et al*., 1982; Jeffrey and Mitra, 1984; Morris *et al*, 1992; Kim and Jhon, 1994; Vorob'ev *et al*., 1996; Deng and Roux, 2004) by various researchers. For L-α-amino acids, L-asparagine, L-cystine, L-glutamic acid, L-lysine, L-proline, L-serine, and L-tryptophan have been found to form hydrates.

The first literature source that described L-serine monohydrate was by Frey and coworkers (1973) in their structure determination of L-serine monohydrate. In their study, L-serine monohydrate crystals were grown at 5 ^{o}C from an aqueous solution saturated at room temperature. They also reported that when the crystals were removed from the solution, they tended to lose water and transform into a white powder. However, the morphology of L-serine monohydrate was not mentioned. A later study done by Charmolue (1990) indicated that the addition of methanol at a high-level of supersaturation would alter the crystal habit of L-serine from hexagonal to needle-like. According to the research conducted by Gatewood (1992), the hexagonal crystals were found to be L-serine monohydrate, while the needle-like crystals were anhydrous L-serine. Based on their results, one could conclude that low temperatures and a low level of methanol would favor the formation of L-serine monohydrate, whereas high methanol concentration favored the formation of anhydrous L-serine.

4.1.2 Experimental Results

4.1.2.1 Validation of Experimental Data

As mentioned in the previous chapter, the conditions of the HPLC column, amount injected, and sensitivity of the detector may not be exactly the same for every run. Error may also be introduced during each sample dilution since the electronic balance is accurate to the nearest 0.1 mg. In order to determine the sensitivity and reproducibility of the HPLC analysis, a total of six random samples were taken from an equilibrium mixture, diluted, derivatized with OPA, and injected into the column for detection. The measured concentrations at equilibrium, as well as the mean and standard deviations are reported in Table 4-1. The variability of data is depicted in Figure 4-1. All data fall within two standard deviations from the mean concentration. Thus, all concentration data determined by HPLC had maximum bounds of ±1.15g per 100 g of water, or a standard deviation of 1.21%. Comparing with the solubility measurements done by Dalton and Schmidt (1935), who had their standard deviation as high as 5.41%, the HPLC analytical method was proved to increase the accuracy of experimental data.

Table 4-1: Analytical results obtained on 6 random samples taken for HPLC analysis

Sample No.	Concentration (g L-Serine/100g Water)
1	47.22
2	47.28
3	47.35
4	46.90
5	48.25
6	48.26
Mean	47.54
Standard Deviation	0.574 (1.21 %)

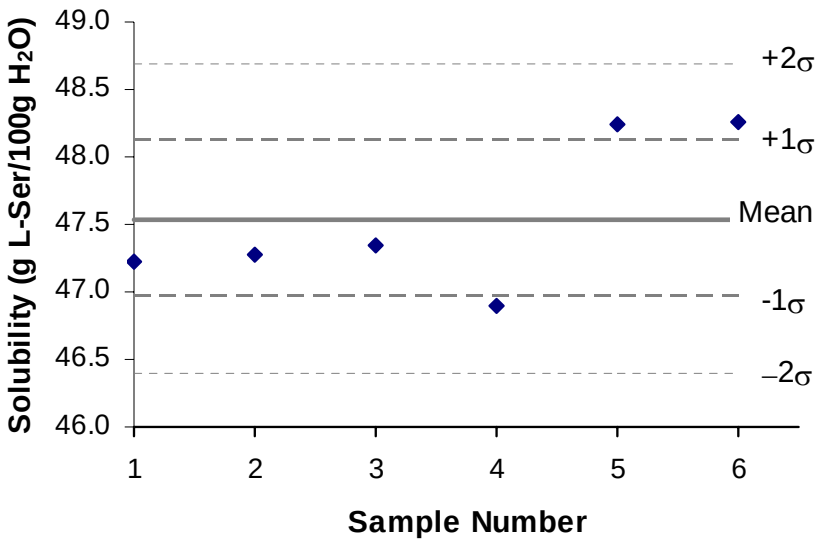

Figure 4-1: Results of the six samples with mean and standard deviations (σ) concentrations shown

4.1.2.2 Solubility

As suggested in Section 4.1.1.2, the pseudo-polymorphic transition between anhydrous L-serine and L-serine monohydrate seems to depend on temperature and methanol concentration. With this in mind, series of solubility experiments that varied both temperature and methanol concentration were performed to examine the effect of temperature and solvent composition on solubility. The existence of a discontinuity in the solubility curves would confirm that the pseudopolymorphs are enantiomorphic; that is, one is more stable than the other over a specific range of temperatures. The experiments also served to expand the literature database in term of the effect of temperature on solubility. The solubilities of L-serine in mixtures of methanol and water were measured over the temperature range 278 K to 333 K. Aqueous solutions containing 0 mol%, 5 mol%, 10 mol%, 16 mol%, and 22 mol% of methanol were prepared at each set of experiments.

The effect of pH on the forms of L-serine present at different solvent compositions was first examined. In general, amino acids can exist as acidic, basic, or zwitterionic form in solution. The isoelectric point for L-serine is 5.68. It exists as the acidic form when the solution pH is less than the isoelectric point, and basic form when the solution pH is more than the isoelectric point. When solution pH is at or near isoelectric point, however, the zwitterionic species is the prevalent form. In the present work, the pH of L-serine in 0 mol%, 16 mol%, and 100 mol% methanol solutions were measured. Their values were 5.73, 5.69, and 5.32 respectively. In any case, over 99.9% was of the zwitterionic form. Hence, it is concluded that L-serine was present in the zwitterionic form in all methanol concentrations studied.

The experimental data are listed in Tables 4-2, 4-3, 4-4, 4-5, and 4-6, and plotted in Figure 4-2 based on the observed morphology (This will be discussed in Section 4-2.). The solid symbols and crosses in Figure 4-2 represent solubility data for systems in which the equilibrated crystals were observed to be hexagonal under an optical microscope. The open symbols and stars represent the solubility data for systems in which the equilibrated crystals were observed to be rod-shaped. Alternatively, the experimental values were arranged to illustrate the solubility isotherms as a function of methanol content, as shown in Figure 4-3.

Table 4-2: Solubility of L-serine in 0 mol% methanol solution

Temperature (K)	Solubility (g L-SER/100g solution)
283.35	19.55
285.85	20.61
289.25	24.37
299.05	30.58
301.05	31.64
315.95	41.70
316.95	41.93
317.75	43.00
322.85	43.89
327.05	45.43

Table 4-3: Solubility of L-serine in 5 mol% methanol solution

Temperature (K)	Solubility (g L-SER/100g solution)
278.25	12.87
283.15	15.53
288.25	18.65
293.15	23.86
298.05	26.93
312.85	35.61
317.85	39.26
322.75	41.55
327.45	43.26
332.45	43.58

Table 4-4: Solubility of L-serine in 10 mol% methanol solution

Temperature (K)	Solubility (g L-SER/100g solution)
283.45	10.28
293.05	16.51
299.95	21.57
302.75	22.61
312.55	27.18
322.55	29.98
332.35	36.10

Table 4-5: Solubility of L-serine in 16 mol% methanol solution

Temperature (K)	**Solubility (g L-SER/100g solution)**
283.25	5.93
285.65	7.01
288.25	8.08
293.05	11.08
302.85	15.43
312.55	19.14
322.55	22.64
332.25	25.98

Table 4-6: Solubility of L-serine in 22 mol% methanol solution

Temperature (K)	**Solubility (g L-SER/100g solution)**
283.35	5.02
291.05	7.45
293.05	7.63
302.85	9.63
312.55	12.15
322.55	15.03
331.55	18.47

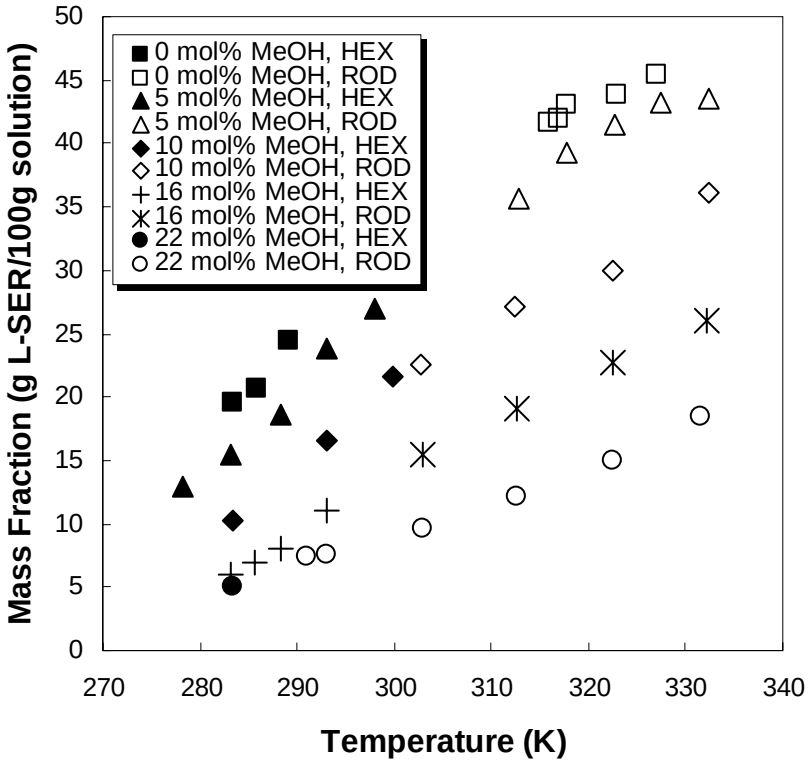

Figure 4-2: Solubility of L-serine in mixed methanol-water system at different temperatures. Solid symbols and crosses represent crystals that were hexagonal; Hollow symbols and stars represent crystals that were rod-shaped

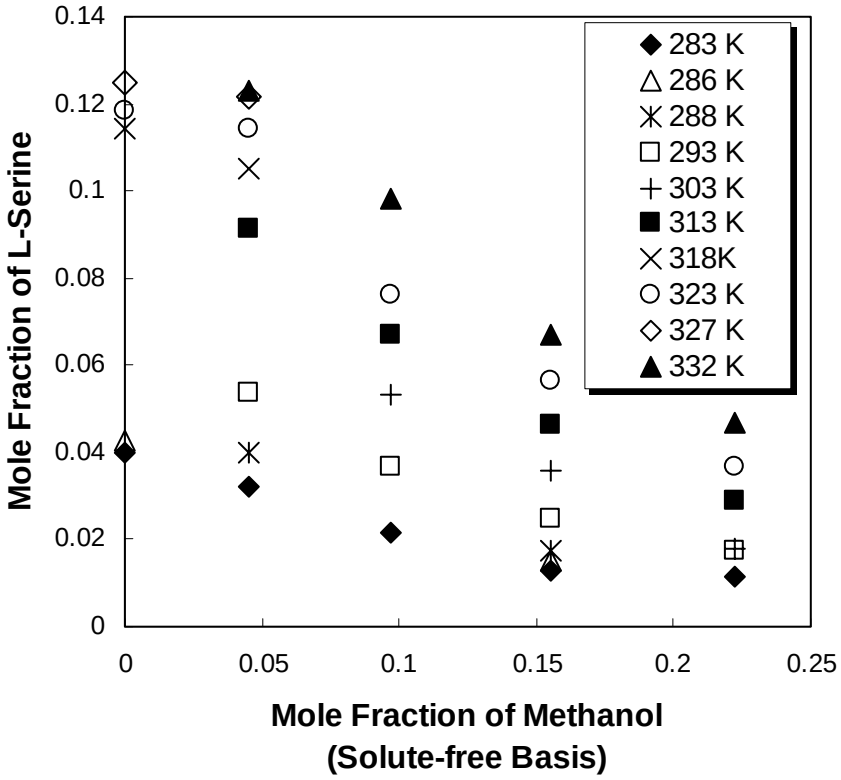

Figure 4-3: Solubility isotherms for L-serine in mixed methanol-water solutions

The influence of temperature and methanol concentration on solubility is clearly illustrated in Figures 4-2 and 4-3. L-serine was most soluble in system containing 0 % methanol, i.e. aqueous solution, at high temperatures. As shown in Figure 4-2, more than 45 g of L-serine could be dissolved into 100 g of solution at 327 K. This could be readily justified since serine had the least hydrophobic side chain among all α-amino acids (Nozaki and Tanford, 1971). When methanol was present, it salted out L-serine quite profoundly. For example, at 323 K, the solubility of L-serine in Figure 4-3 was reduced to 1/4 of the value in 22 mol% methanol compared to that in pure water. As expected, the solubility of L-serine decreased with a decrease in temperature. However, the dependence of solubility in these mixed solvent systems changed quite significantly with

temperature. When the solution mixture was cooled, solubility decreased to a smaller degree at higher methanol concentrations. With that, the effects of temperature and methanol concentration on solubility are summarized in Table 4-7.

Table 4-7: Effect of temperature and methanol concentration on solubility of L-serine

Solubility	Low Temperature	High Temperature
Low Methanol Concentration	Higher	Highest
High Methanol Concentration	Lowest	Lower

Next, the transition from one stable pseudo-polymorph to another was investigated by looking for possible discontinuities in the solubility curves. It is not easy to detect discontinuities in the data of Figure 4-2, by visual inspection in 0 mol% and 5 mol% methanol solutions. However, in systems of 10 mol%, 16 mol%, and 22 mol% methanol, the slopes of the solubility curves clearly were steeper in regions where the hexagonal crystals were formed than those in the region of rod-shaped crystals. Also, the open symbols and stars occupied a larger temperature range with increase in methanol concentrations. Based on the observed morphology, as discussed in Section 4.2, and the discontinuities in the solubility curves, the transition between anhydrous and monohydrate forms of L-serine is further analyzed in the next section.

When possible, the solubility data measured in this study were compared with the values available in the literature and the results are shown in Table 4-8. They were in good agreement at most values at 283 K. A largest discrepancy was found for the solubility in 22 mol% solution at 283 K (20.5 %). The result of this study had a solubility of 29.219 g of L-serine in 100 g of water, which was 16.7% higher than the literature

value. It was important to note that although only one measurement was taken, the reproducibility of the HPLC measurements were confirm based on six independent measurements (The standard deviation was found to be 1.21 %, see Section 4.1.1). Possible sources of discrepancy were lack of mentioning of agitation of the solution mixture, and temperature fluctuation during sample filtration in the literature experimental method.

Table 4-8: Comparison of solubility data for L-serine in mixtures of water and methanol
[1] Hade (in Fasman, 1976); [2] Charmolue (1991)

Methanol Composition		**Mass Ratio (g L-serine/100g solute-free solvents)**			
		283 K	**Deviation**	**303 K**	**Deviation**
0 mol%	this work	24.30		—	
	literature[1]	24.70	1.7 %	47.60	—
	literature[2]	22.72	6.5 %	39.41	—
5 mol%	this work	18.38		—	
	literature[2]	18.90	3.3 %	33.04	—
		19.06		33.90	
10 mol%	this work	11.45		29.22	
	literature[2]	11.58	1.1 %	24.38	16.7 %
		11.59		24.28	
16 mol%	this work	6.30		18.25	
	literature[2]	5.95	1.8 %	16.90	7.5 %
		6.88		16.87	
22 mol%	this work	5.29		10.65	
	literature[2]	3.96	20.5 %	9.26	16.0 %

4.1.2.3 Transition between Anhydrous and Monohydrate Forms

As indicated in the previous Section, discontinuities in solubility data were suspected for the curves presented in Figure 4-2. To test this notion, empirical fits were applied to all solubility curves. Exponential fits were applied to the solubilities when hexagonal L-serine (monohydrate) crystals were formed and to the solubilities when rod-shaped (anhydrous) L-serine crystals were formed. The results are shown in Figure 4-4. The solubility curves for the monohydrate form and the anhydrous form at the same methanol concentration were connected by extrapolation to aid in visualization.

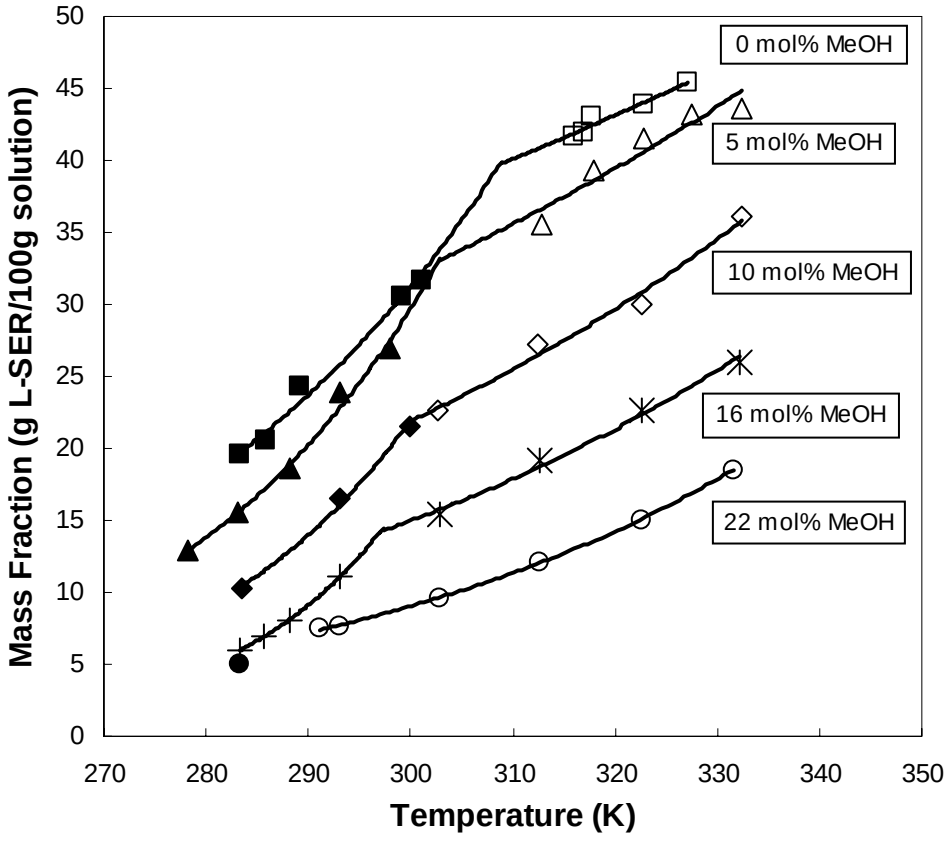

Figure 4-4: Empirical fits to the solubility data in mixed methanol-water solutions. Solid symbols and crosses represent L-serine monohydrate. Hollow symbols and stars represent anhydrous L-serine

The empirical exponential functions were found to be good fits for all solubility data, with coefficients of correlation (R^2) above 0.91. With the exception of 40 vol% methanol solution, which contain only one point for the solubility of L-serine monohydrate, all solubility curves experienced breaks at various methanol concentrations.

An important observation from the results is that no data in the literature had reported the transition of L-serine. While the effect of methanol on the solubility of L-serine had been known, the effect on the temperature at which there is a transition from one stable species to another had not been explored. For instance, the temperature at which the solubility curves of L-serine monohydrate and anhydrous L-serine crossed should be the transition temperature. In the case of pure water system, the transition temperature was approximated to be close to 40 ^{o}C. A thermodynamic model is to be used in section 4.1.3 to evaluate the exact transition temperatures for different methanol contents, though it could be safely assumed, judging from the break points in Figure 4-3, that the transition temperatures seemed to decrease with an increase in methanol content.

When solubility isotherms were constructed as a function of solvent compositions, the data can be separated by a line where the pseudo-polymorphic outcomes are inferred qualitatively. An illustrative plot is shown in Figure 4-5. Based on the analysis of crystals, all data at 283 K, 286 K, and 288K, and data of mole fractions of 0.046, 0.099, 0.158 at 293 K were known to be operated under the monohydrate regime, while the rest were operated under the anhydrous regime. These data were approximately divided by a straight line. All data points situated below the line represented the solubility data of L-serine monohydrate. Hence if temperature and

methanol concentration were controlled at this regime, L-serine monohydrate crystals were always expected. On the other hand, all data point situated above the line represented the solubility data of anhydrous L-serine. If we operated in this regime, anhydrous L-serine crystals were the expected outcome. It was, however, important to note that these guidelines served only for qualitative purpose. More data points, especially at higher mole fractions of methanol, would be necessary to decide on an appropriate fit for the fictitious operating line and therefore the quantitative outcomes of such pseudo-polymorphic transitions.

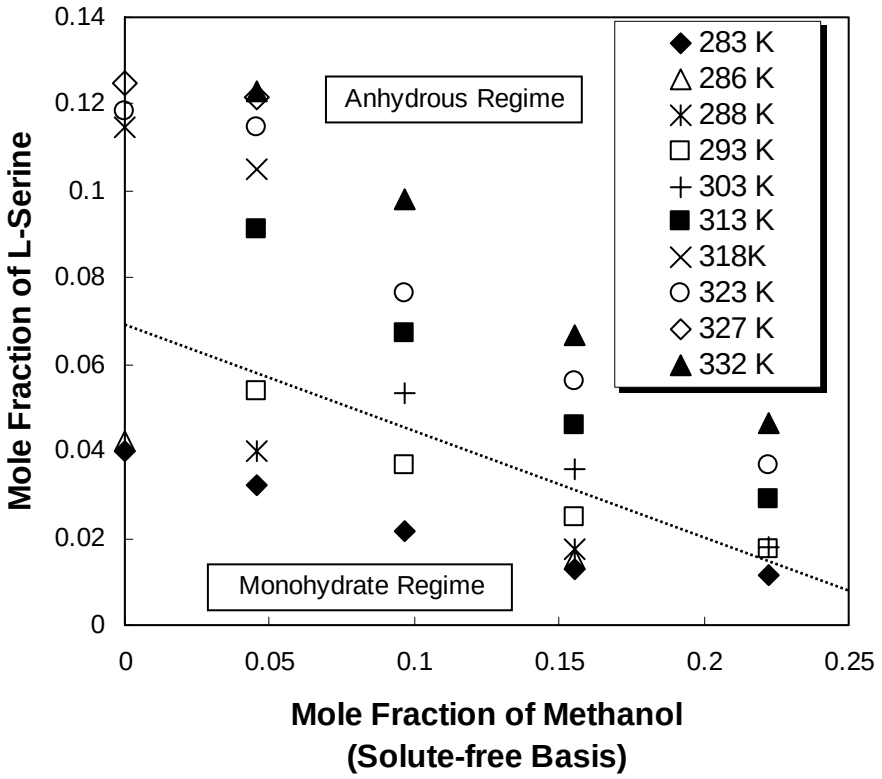

Figure 4-5: Pseudo-polymorphic outcomes for L-serine in water-methanol systems

4.1.3 Solubility Model

4.1.3.1 Development

The thermodynamic framework for the solubility of solids in liquids has been outlined by Prausnitz *et al*. (1999). At equilibrium, the fugacity of the solute (an amino acid in the present case) in its pure solid form is equal to the fugacity of the solute in liquid solution:

$$f_{i,\text{pure solid}} = f_{i,\text{solute in liquid solution}} \tag{4.1}$$

where component i is the amino acid solute. The fugacities of the amino acid in the liquid and solid phases can be written as

$$f_{i,\text{solute in liquid solution}} = x_i \gamma_i f_i^L \tag{4.2}$$

$$f_{i,\text{pure solid}} = f_i^S \tag{4.3}$$

where x_i is the mole fraction of the amino acid in the liquid solution (the solubility), γ_i is the liquid phase activity coefficient, and f_i^L is the reference-state fugacity, which can be defined as the pure subcooled liquid amino acid at the temperature of the solution. Therefore,

$$\ln\left(\frac{f_i^L}{f_i^S}\right) = \ln\left(\frac{1}{x_i \gamma_i}\right) \tag{4.4}$$

The Gibbs energy change for the solute dissolution process at temperature T is related to the fugacities of the solid and subcooled liquid by

$$\Delta g = RT \ln \frac{f_i^L}{f_i^S} \tag{4.5}$$

Because the Gibbs energy is a state function, it can be evaluated using the thermodynamic cycle depicted in Figure 4-6.

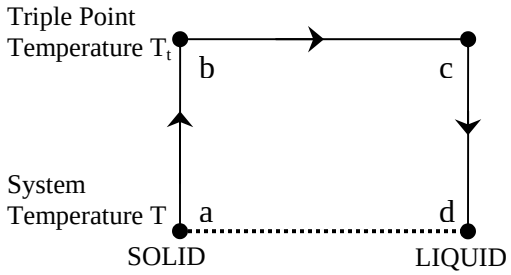

Figure 4-6: Thermodynamic cycle for calculating the Gibbs energy change

First, the amino acid at solid state at a temperature, T, is heated to its triple point temperature, T_t (a → b). Second, an isothermal phase change from solid to liquid state occurs at the triple point temperature (b → c). Finally, the liquid phase amino acid at T_t is cooled to T. The Gibbs energy change is related to the corresponding enthalpy and entropy changes by

$$\underset{a\to d}{\Delta g} = \underset{a\to d}{\Delta h} - T \underset{a\to d}{\Delta S} \tag{4.6}$$

$$\underset{a\to d}{\Delta h} = \underset{a\to b}{\Delta h} + \underset{b\to c}{\Delta h} + \underset{c\to d}{\Delta h} \tag{4.7}$$

$$\underset{a\to d}{\Delta s} = \underset{a\to b}{\Delta h} + \underset{b\to c}{\Delta h} + \underset{c\to d}{\Delta h} \tag{4.8}$$

Eqns. (4.7) and (4.8) can be rewritten in terms of heat capacity c_p and enthalpy of fusion, $\Delta_{\text{fus}} h$:

$$\underset{a\to b}{\Delta h} = \int_{T}^{T_t} c_{p(\text{solid})} dT;\ \underset{a\to b}{\Delta s} = \int_{T}^{T_t} \frac{c_{p(\text{solid})}}{T} dT \tag{4.9}$$

$$\underset{b\to c}{\Delta h} = \Delta_{\text{fus}} h_{\text{at T}_t};\ \underset{b\to c}{\Delta s} = \frac{\Delta h^{\text{fus}}}{T_t} \tag{4.10}$$

$$\underset{c\to d}{\Delta h} = \int_{T_t}^{T} c_{p(\text{liquid})} dT;\ \underset{c\to d}{\Delta s} = \int_{T_t}^{T} \frac{c_{p(\text{liquid})}}{T} dT \tag{4.11}$$

Substitution of Eqns. (4.6), (4.7), (4.8), (4.9), (4.10), and (4.11) into Eqn. (4.5) with rearrangement yields the following expression:

$$\ln\left(\frac{1}{x_i \gamma_i}\right) = \frac{\Delta_{\text{fus}} h}{R T_t}\left(\frac{T_t}{T} - 1\right) - \frac{\Delta c_p}{R}\left(\frac{T_t}{T} - 1\right) + \frac{\Delta c_p}{R} \ln \frac{T_t}{T} \tag{4.12}$$

where $\Delta c_p = c_{p(\text{liquid})} - c_{p(\text{solid})}$

Eqn. (4.12) is the general expression that is used to relate solubility data to system temperature. It is important to note that the right-hand side of the equation is a function of the physical properties of the solute only. The influence of solvents on solute solubility is accounted for by the activity coefficient, γ_i. Appropriate activity coefficient models such as Wilson, Margules, NRTL (**N**on-**R**andom-**T**wo-**L**iquid), or UNIQUAC (**UNI**versal **QUA**si-**C**hemical)-type equations are usually used in such correlations.

4.1.3.2 Solubility Data Correlations

Modeling of the solubilities of amino acids in mixed-solvent systems has been known to present considerable challenges. First, the physical properties ($\Delta_{\text{fus}}h$, T_t, and Δc_p) of amino acids in Eqn. (4.12) are typically measured or estimated. Since serine decomposes at temperatures below its melting point, these physical property data are not available in the literature and cannot be measured easily. Furthermore, models for activity coefficients are more complex because ternary interaction parameters or additional binary interaction parameters may be required.

Orella and Kirwan (1991), Gude *et al*. (1996 a, b), and Ferreira *et al*. (2004) attempted to correlate solubility data using an excess solubility approach, instead of the usual thermodynamic cycle method described in the previous section. Details of the methods of Orella and Kirwan, and Gude *et al*. were outlined in Section 2.3 of Chapter 2. The model presented by Gude and coworkers is the simplest, with only one ternary Margules interaction parameter. However, their method had an average relative deviation of 27.7 % even when applying to water-methanol systems, which are considered the easiest to correlate. Solubility data correlated using the method developed by Orella and Kirwan had an average relative deviation of 15 %, but more parameters were necessary. Ferreira and coworkers correlated the solubility data of glycine and dl-alanine in aqueous systems of ethanol, propanol, and isopropanol with smaller average relative deviation of 8.4 %. However, an attempt to introduce a temperature dependence parameter to the model was less successful.

Based on these observations, a simple solubility model will be used here to correlate the solubility data of L-serine as a function of temperature in mixed water-

methanol systems. Starting from Eqn. (4.12), three assumptions were made. First, the difference between the triple-point temperature and melting temperature is assumed to be small; also, the difference in the enthalpies of fusion at these two temperatures is taken to be negligible. Hence, as is common practice, we substitute the normal melting temperature, T_m, for T_t and to use the enthalpy of fusion at T_m. Second, the difference in the heat capacity of the solute in its solid-state and in its liquid-state, Δc_p, is relatively small. Therefore to a fair approximation, the second and third terms on the right-hand side of Eqn. (4.12) can be neglected. Third, the activity coefficient approach is not used to account for the non-ideality of the solution in this model. With these approximations, Eqn. (4.12) can be re-written as:

$$\ln x_i = -\frac{\Delta H_f}{RT} + \frac{\Delta H_f}{RT_m} \tag{4.13}$$

This is known as the van't Hoff equation. Also, $\Delta H_f = T_m \Delta S_f$, where ΔS_f is the entropy of fusion.

Beiny and Mullin (1987) suggested an excess approach to capture the non-ideality of the solution by replacing the enthalpy of fusion ΔH_f with enthalpy of dissolution ΔH_d, which incorporates the excess enthalpy of mixing, and ΔS_f by ΔS_d. The excess enthalpy and entropy of mixing are terms that result from the interaction of the molecules of different shape and size. Hence, Eqn. (4.13) becomes:

$$\ln x_i = -\frac{\Delta H_d}{RT} + \frac{\Delta S_d}{R} \tag{4.14}$$

Using Eqn. (4.14) as a guide, mole fractions of anhydrous L-serine and L-serine monohydrate were plotted in a logarithmic scale against the reciprocal of the absolute

temperature for each water-methanol system. The enthalpy and entropy of dissolution can be obtained from the slope and the intercept of the straight line, respectively. The results of these correlations are shown in Figure 4-7. Correlations of solubility data for individual water-methanol system are shown in Figures 4-8, 4-9, 4-10, 4-11, and 4-12.

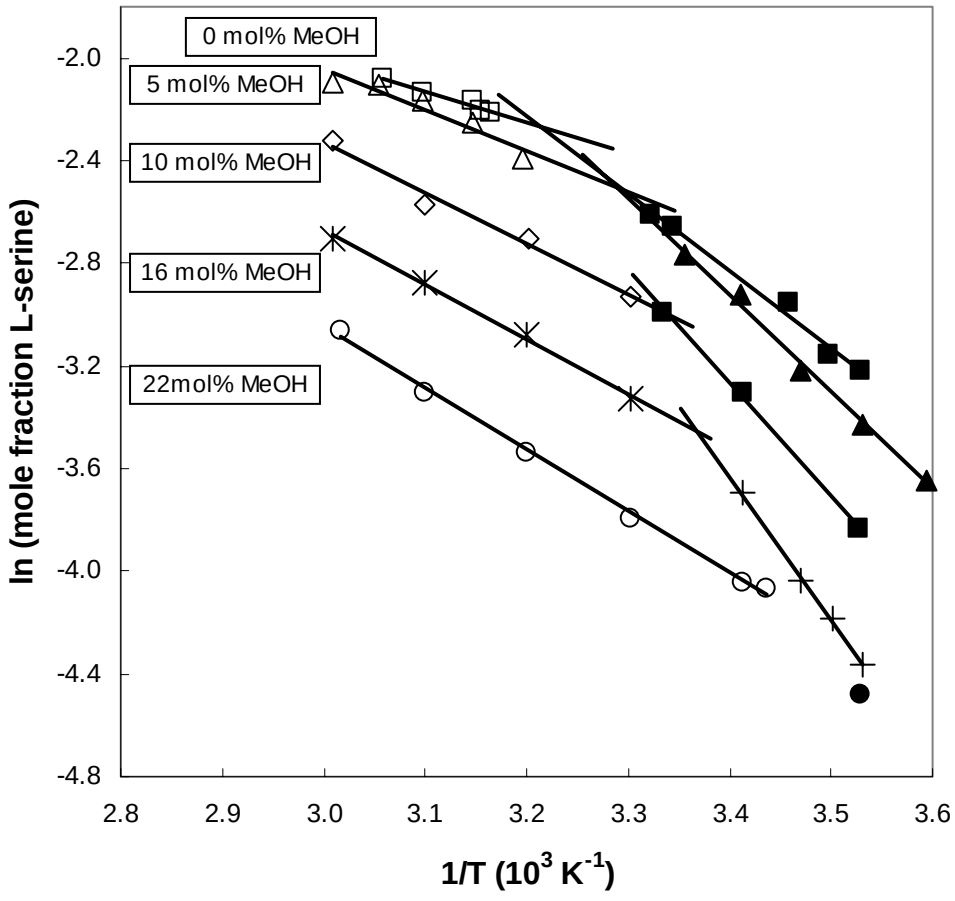

Figure 4-7: Correlation of anhydrous L-serine and L-serine monohydrate solubility data in different water-methanol system. The open symbols and stars represent data for the anhydrous form while the solid symbols and crosses represent data for the monohydrate form. Straight lines are fitted to the data with extrapolation

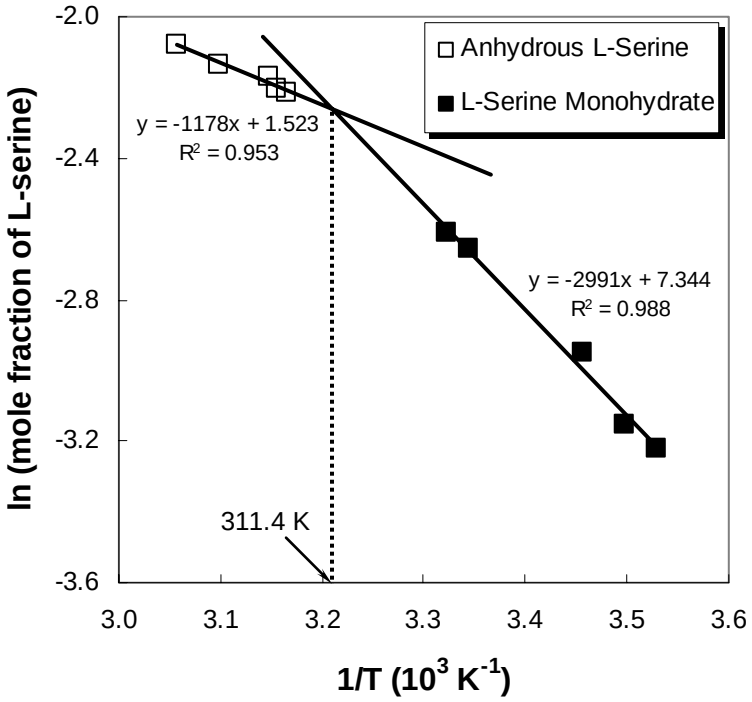

Figure 4-8: van't Hoff plot for the correlation of solubility data in 0 mol% methanol solution

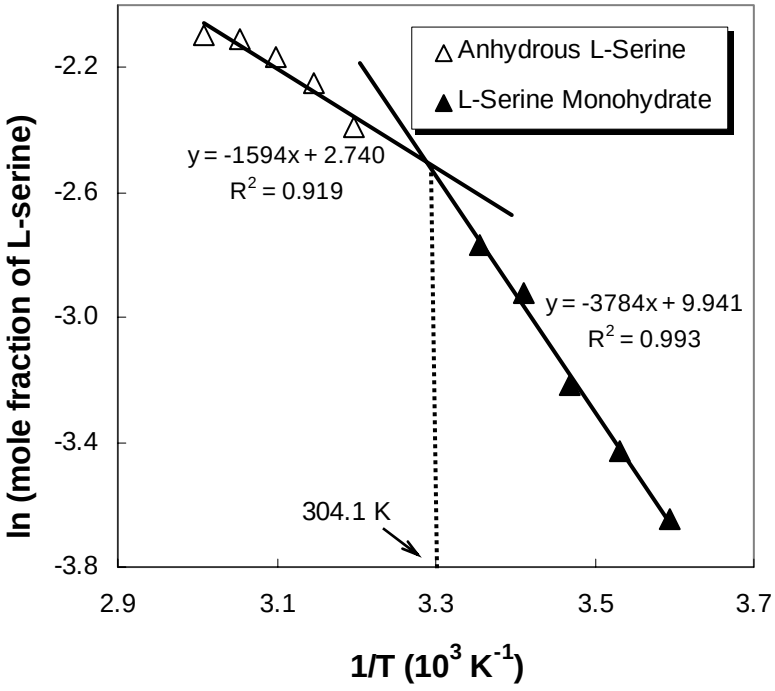

Figure 4-9: van't Hoff plot for the correlation of solubility data in 5 mol% methanol solution

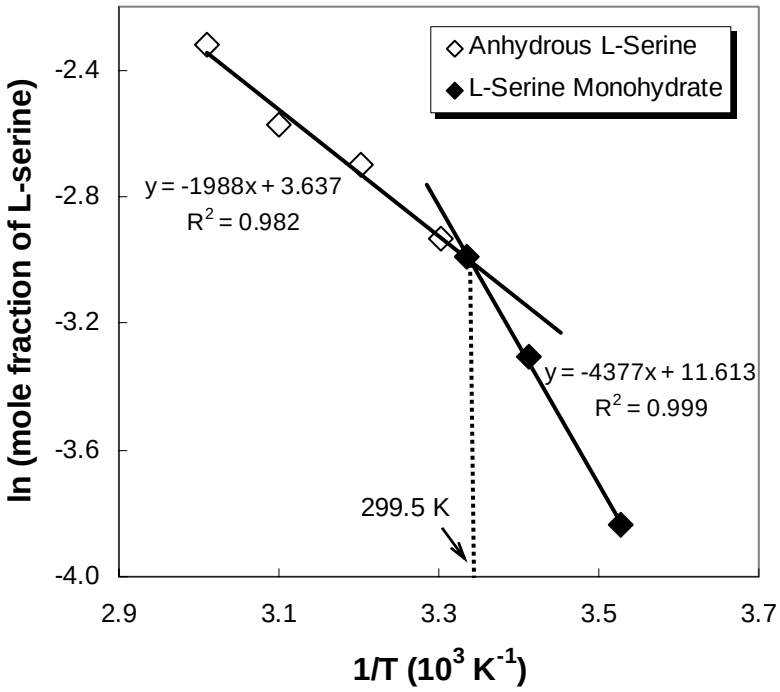

Figure 4-10: van't Hoff plot for the correlation of solubility data in 10 mol% methanol solution

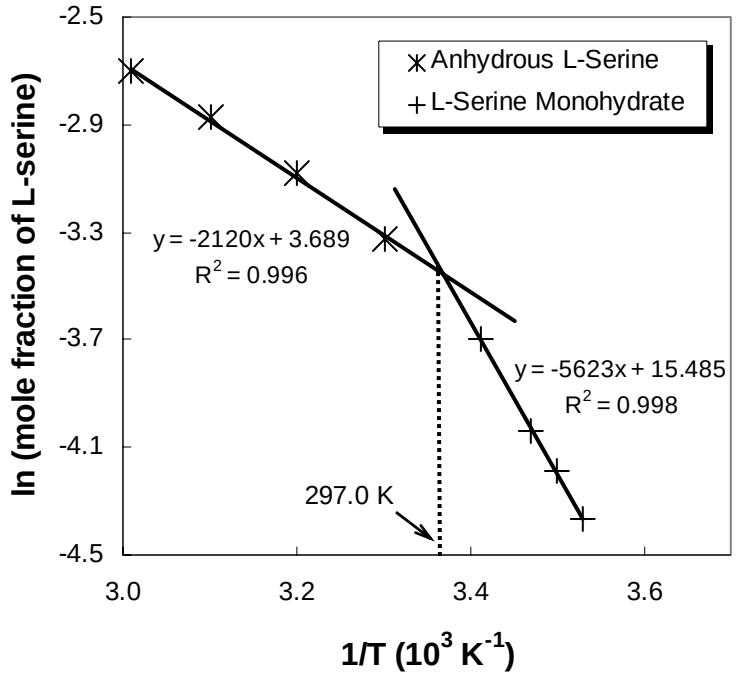

Figure 4-11: van't Hoff plot for the correlation of solubility data in 16 mol% methanol solution

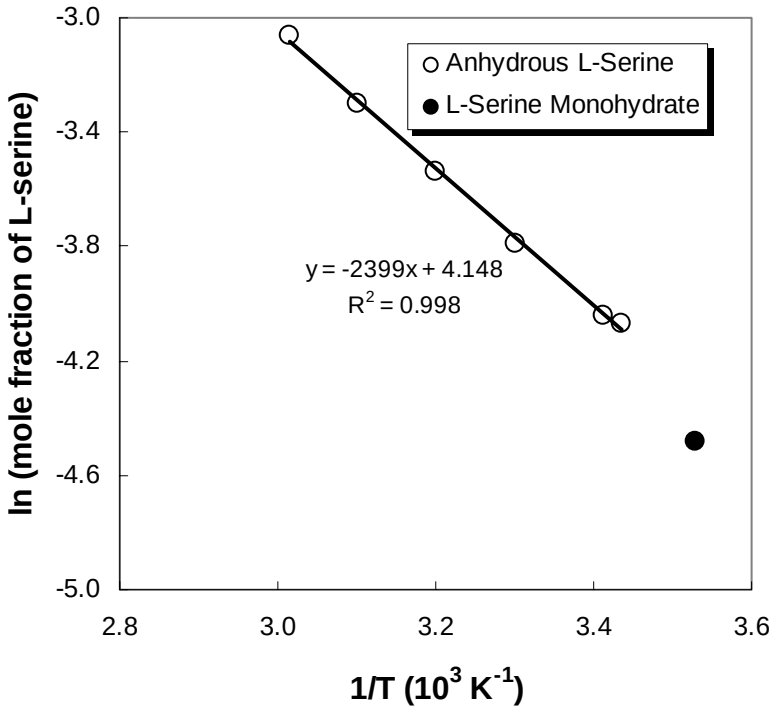

Figure 4-12: van't Hoff plot for the correlation of solubility data in 22 mol% methanol solution

In general, the solubility correlations agreed well with the experimental data: linearity was observed when solubility data were plotted as ln x versus 1/T; straight lines were sufficient to correlate all solubility data with good fits, except in the case of anhydrous L-serine in 5 mol% methanol. Furthermore, the quality of correlation increased with higher temperature range. For example, the solubility data for L-serine in pure water merely covered a temperature range of 11 K, while the temperature range of solubility data in 22 mol% methanol was 41 K. As a result, the correlation coefficient increased from 0.953 in the case of pure water to 0.998 in 22 mol% methanol. The temperature range of the solubility data, however, is limited by the temperature at which there is a transition between more stable forms of the pseudo-polymorphs.

As observed in the figures, the slopes of van't Hoff plots increased with methanol concentration. For instance, the slope of the line for anhydrous L-serine is -1178 in 0 mol% methanol solution. The slope becomes steeper at higher mol% methanol. Eventually, at 22 mol% methanol, the value is -2399.

4.1.3.3 Determination of Parameters

Table 4-9 lists the values for the enthalpy and entropy of dissolution for different water-methanol systems.

Table 4-9: Dissolution parameters for L-serine in different water-methanol systems

	0 mol% MeOH		**5 mol% MeOH**		**10 mol% MeOH**		**16 mol% MeOH**		**22 mol% MeOH**	
cal/mol	ΔH_d	ΔS_d	ΔH_d	ΔS_d	ΔH_d	ΔS_d	ΔH_d	ΔS_d	ΔH_d	ΔS_d
L-SER	2343	3.03	3167	5.44	3950	7.23	4213	7.33	4767	8.24
L-SER· H_2O	5945	14.60	7519	19.76	8697	23.08	11173	30.77	—	—

ΔH_d (from calorimetry) in water at 25 ^oC (L-SER) = 2.8 kcal/mol (Fasman, 1976)
ΔH_d (from solubility data) in water at 25 ^oC (L-SER· H_2O) = 4.6 kcal/mol (Fasman, 1976)

Enthalpy and entropy of dissolution for each water-methanol system were calculated from the slope and intercept using Eqn. (4.14). As made clear in Figure 4-6, the slopes of the lines for L-serine monohydrate were greater than those for anhydrous L-serine. Therefore, the values of the enthalpy of dissolution were higher for L-serine monohydrate, as shown in Table 4-9. Moreover, the enthalpy of dissolution increased with increased mole percent of methanol. The same is true for the entropy of dissolution. For instance, the entropy of dissolution was 90 % higher in 16 mol% methanol than in 0 mol% methanol. The reason for this behavior is that L-serine is almost insoluble in pure methanol. According to the study by Charmolue (1991), only around 0.703 g of L-serine can be dissolved in 100-mL of pure methanol. Hence, more energy is required to dissolve L-serine with increasing methanol concentration.

Table 4-9 lists the enthalpies of dissolution of L-serine and L-serine monohydrate in water at 25 ^{o}C from Fasman (1976) for comparison. Value of the enthalpy of dissolution of anhydrous L-serine in Fasman (2.8 kcal/mol) is greater than this work (2.3 kcal/mol). However, it is clearly stated in the literature that enthalpy of hydration was not accounted for in the reported value, as L-serine only exists as the monohydrate form under the conditions. So the actual enthalpy of dissolution is expected to be lower and in closer agreement with the value of this work. Enthalpy of dissolution of L-serine monohydrate in this work is 23 % higher than the reported value. The large difference is due to the approximation that the enthalpy of dissolution is invaried within the temperature range of this study. Attempt has been made to correlate only the solubility data at 299.05 K (25.9 ^{o}C) and 301.05 K (27.9 ^{o}C) for L-serine monohydrate in 0 mol%

methanol, which resemble the temperature of the reported data more closely. This resulted in a value that is in closer agreement with the reported value (4.1 kcal/mol).

The transition temperatures between stable pseudo-polymorphs were determined from the van't Hoff plots by extrapolation of the solubility data until the line of the hydrated form and anhydrous form cross. The results for 0 mol%, 5 mol%, 10 mol%, and 16 mol% methanol are represented in Figures 4-7, 4-8, 4-9, and 4-10 respectively. The transition temperature for 22 mol% methanol could not be determined because there is only one data point for the solubility of L-serine monohydrate. It is shown from Figure 4-6 that the intersection of the monohydrate line and anhydrate line shifts to the right with increasing methanol concentration. In other words, the transition temperature decreased with an increase in methanol concentration. This is confirmed when the transition temperature is plotted against solvent composition in Figure 4-13. The transition temperatures are listed in Table 4-10.

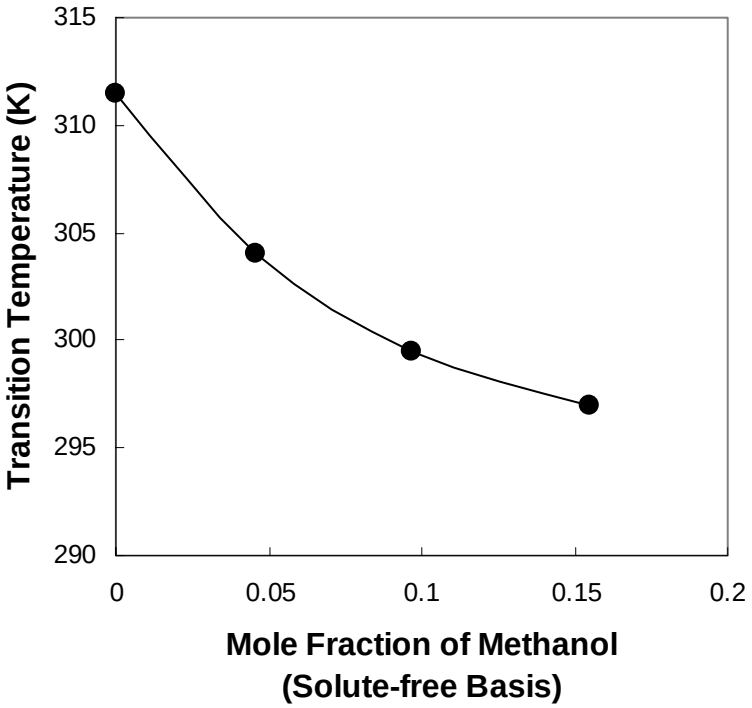

Figure 4-13: Change in transition temperature with solvent composition

Table 4-10: Transition temperatures between anhydrous L-serine crystals and L-serine monohydrate crystals

Methanol Concentration	Transition Temperature (K)
0 mol %	311.4
4.55 mol %	304.1
9.68 mol %	299.5
15.52 mol %	297.0

4.2

Morphology and Analysis of L-Serine Crystals

4.2.1 Observed Morphology

Crystal morphology was observed under an optical microscope prior to each sampling of solution and at the completion of each set of solubility experiments. The former served to ensure the accuracy of solubility measurements by confirming that the system had reached equilibrium; in other words, at equilibrium only one crystal form should be present. The latter was performed to prepare solid samples for powder X-ray diffraction. Experimental procedures are described in Section 3.2.1. The following sections address the interesting phenomena observed during the analysis of L-serine morphology.

4.2.1.1 Transition Between Crystal Forms

L-serine crystals undergo pseudo-polymorphic transition from the anhydrous (rod-shaped) form to the monohydrate (hexagonal) form during cooling re-crystallization of the solution mixture. The following details the change in morphologies of L-serine crystals with temperatures at each water-methanol system.

Pure Water: All crystal samples taken at 327, 323, 318, 317, and 316 K appeared to be anhydrous L-serine, while those collected at 301, 299, 289, 286, and 283 were L-serine monohydrate. Optical photomicrographs of the anhydrous form and monohydrated form of L-serine crystals are shown in Figures 4-14 (a) and 4-15 (a) respectively.

5 mol% Methanol: Samples taken at temperatures of 332, 328, 323, 318, and 313 K were of the anhydrous form. A typical optical photomicrograph of the anhydrous L-serine crystals is shown in Figure 4-14 (b). Samples taken at 298, 293, 288, 283, and

278 K were of the hydrated form. A close-up view of a monohydrated L-serine crystal is shown in Figure 4-15 (b). No major cracks or liquid pockets on the crystal surface was observed. Hence solvent inclusion or impurity incorporation was believed to be minimal.

10 mol% Methanol: The crystal samples changed from the rod-like anhydrous form at high temperatures (332, 323, 313, and 303 K), shown in Figure 4-14 (c), to plate-like monohydrated form at lower temperatures (300, 293, and 283 K), shown in Figure 4-15 (c). The crystals shown in Figure 4-14 (c) are more elongated than those from pure water (Figure 4-14 (a)) and 5 mol% methanol (Figure 4-14 (b)).

16 mol% Methanol: Samples taken at 332, 323, 313, and 303 K were anhydrous L-serine crystals. A close-up view of crystals of such form is shown in Figure 4-14 (d). On the other hand, samples taken at 293, 288, 286, and 283 K were L-serine monohydrate crystals. Optical photomicrograph of L-serine monohydrate crystals at 288 K is presented in Figure 4-15 (d).

22 mol% Methanol: Crystal samples changed from the anhydrous form at temperatures of 332, 323, 313, 303, 293, and 291 K to the monohydrated form at 283 K. Representative micrographs for the two crystal forms are shown in Figures 4-14 (e) and 4-15 (e). Both forms appear to be significantly different from what was observed at lower methanol concentrations. The rod-like shape of the anhydrate form has been modified to a more needle-like shape, and the angles of the hexagonal plates of the monohydrate have become more rounded. Clearly, these effects must be related to the methanol concentration in the solution from which the crystals were grown.

The shape of a crystal is determined by the relative rates of deposition on its various faces; the general rule is that faces that grow slowest appear as the largest

developed faces. Khoshkhoo and Anwar (1993), and Berkovitch-Yellin (1985) have studied the effect of solvent on crystal morphology. Their work indicates that solvent affects the habit of crystals through selective adsorption of solvent molecules on specific crystal faces, and the need to remove the solvation layer prior to deposition of oncoming crystal layers causes retardation of growth of these faces relative to growth of other faces. Therefore, it is possible to speculate that methanol molecules selectively adsorb on the elongated faces of the anhydrous L-serine crystals. In order to remove the additional solvation layers, the growth of these faces becomes slower relative to others. When the concentration of methanol increases, more methanol molecules are available to deposit on the elongated faces, thereby inhibiting the growth of these faces further. As a result, anhydrous L-serine crystals adopt a more needle-like morphology at higher methanol concentration.

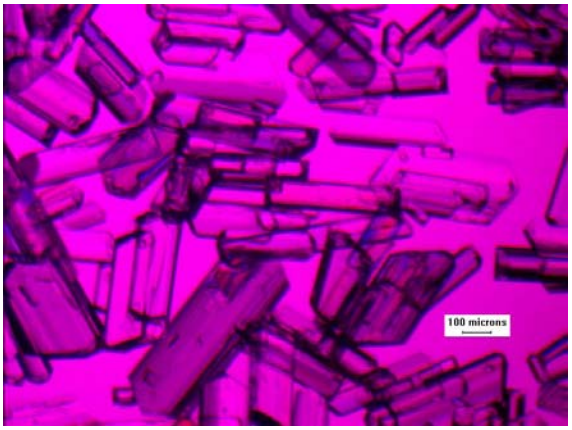

(a) 0 mol% methanol solution at 318 K (4X magnification)

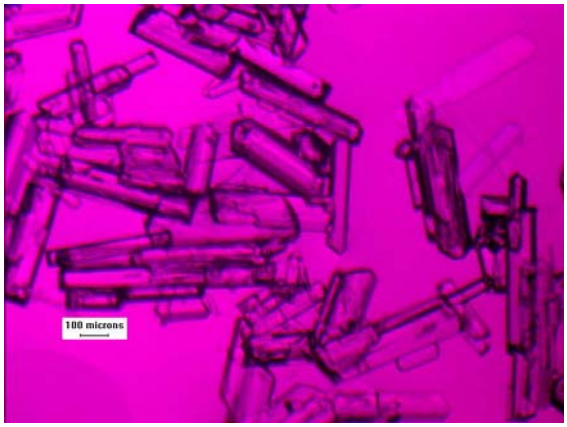

(b) 5 mol % methanol solution at 332 K (4X magnification)

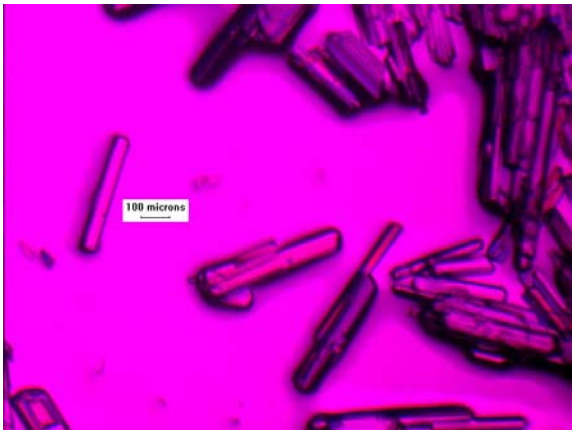

(c) 10 mol% methanol solution at 332 K (4X magnification)

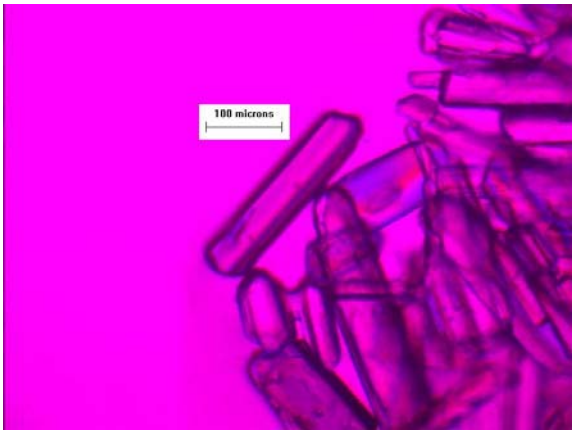

(d) 16 mol% methanol solution at 332 K (10X magnification)

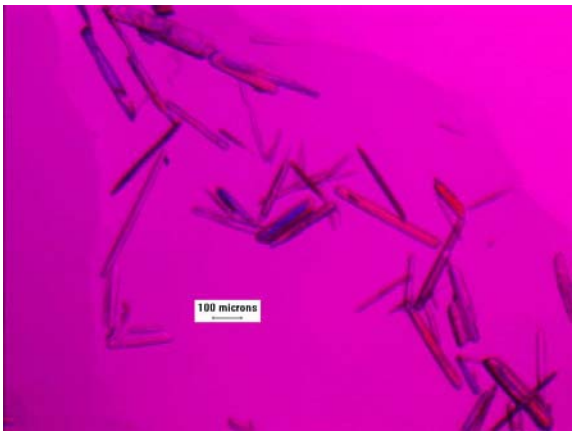

(e) 22 mol% methanol solution at 332 K (4X magnification)

Figure 4-14: Photomicrographs of anhydrous L-serine crystals in (a) 0 mol%, (b) 5 mol%, (c) 10 mol%, (d) 16 mol%, and (e) 22 mol% methanol solutions

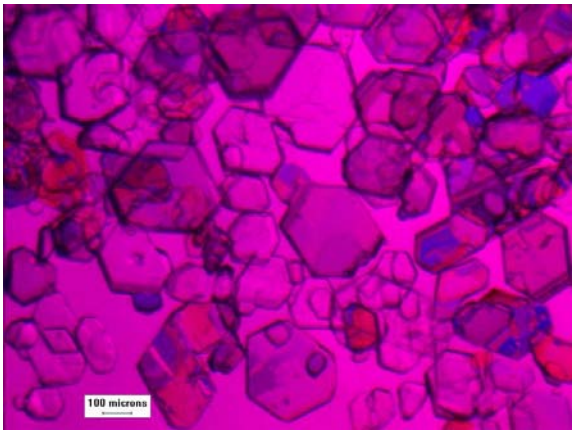

(a) 0 mol% methanol solution at 299 K (4X magnification)

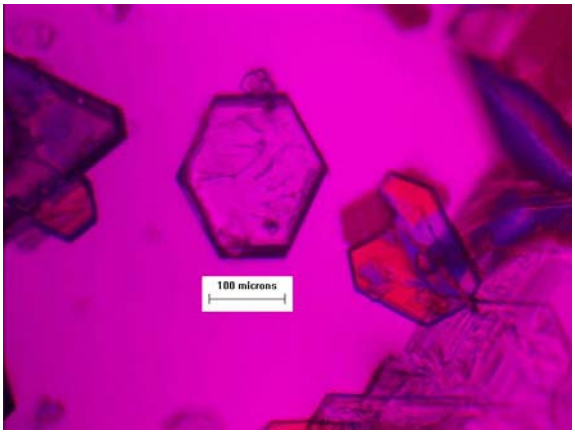

(b) 5 mol% methanol solution at 298 K (10X magnification)

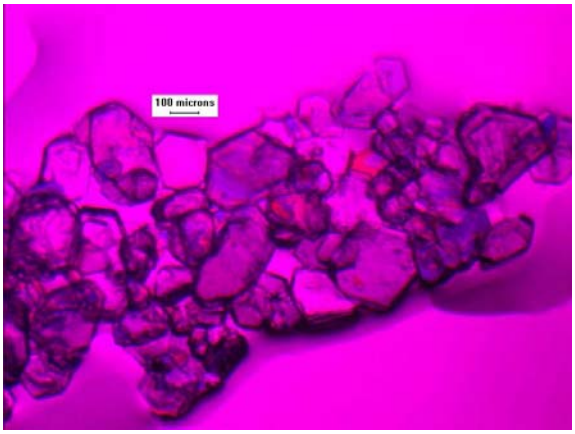

(c) 10 mol% methanol solution at 283 K (4X magnification)

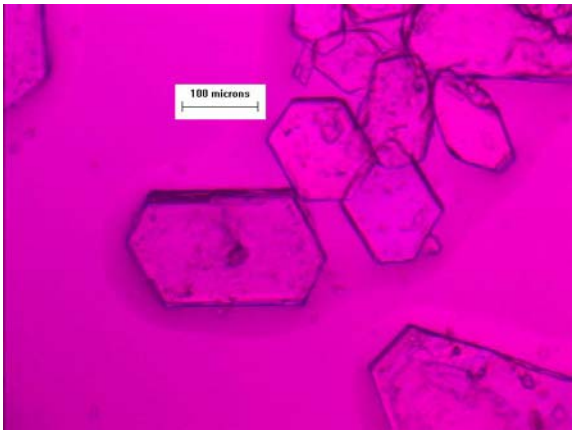

(d) 16 mol% methanol solution at 288 K (10X magnification)

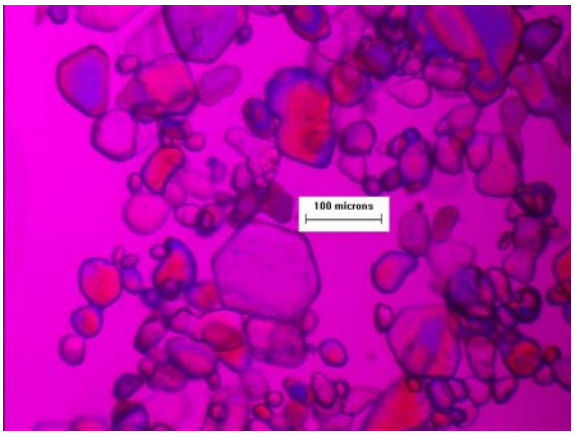

(e) 22 mol% methanol solution at 283 K (10X magnification)

Figure 4-15: Photomicrographs of L-serine monohydrate crystals in (a) 0 mol%, (b) 5 mol%, (c) 10 mol%, (d) 16 mol%, and (e) 22 mol% methanol solutions

4.2.2 Structural Analysis of L-serine Crystals

4.2.2.1 Anhydrous L-serine Crystals

The rod-shaped L-serine crystals were analyzed to confirm that they are the anhydrous form. Pure L-serine crystals from the manufacturer were rod-shaped when viewed under optical microscope (Figure 2-2 in Section 2.1). Therefore, they were used in the powder X-ray diffraction analysis. Analytical procedures are discussed in Section 3.2.2. The resulting diffraction intensity pattern is shown in Figure 4-16 along with the calculated pattern from Cerius^2 and experimental peak data from the ICDD database of anhydrous L-serine. The parameters from the single-crystal data by Kistenmacher and coworkers (1974) were input to Cerius^2 to calculate the powder pattern. Relative intensities were used in the analysis which took the largest peak intensity as a reference. All other intensities were calculated relative to the largest peak.

As seen in Figure 4-29, except at high Bragg's angle, the calculated patterns had almost identical peak positions with the experimental data from ICDD. The peak positions in the diffraction are especially important because the d-spacing (d_{hkl}) between the lattice planes of a crystal can be calculated from the Bragg's angle. The relationship between the Bragg's angle, 2θ, and d-spacing of the corresponding lattice plane can be written as:

$$n\lambda = 2d_{hkl}\sin\theta_{hkl} \qquad \textit{Eqn } 4.1$$

where λ is the wavelength of the radiation source, and n is an integer.

The peak positions of the sample were found to be in good agreement with the calculated pattern and the peak data from the ICDD database. Hence, it was confirmed

that the L-serine crystals from the manufacturer were indeed the anhydrous form. Also, the data confirm that the rod-shaped crystals belonged to the anhydrous form of L-serine, consistent with the study reported by Gatewood (1992).

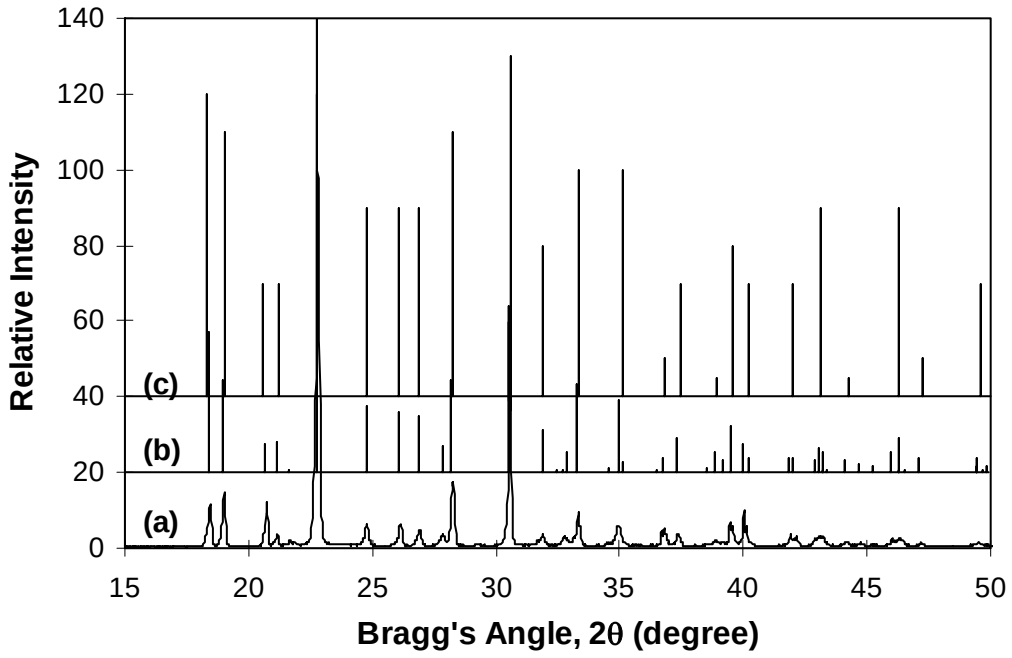

Figure 4-16: Comparison of the powder X-ray intensities. (a) Powder pattern of the pure L-serine crystals; (b) Calculated peak data of anhydrous L-serine from Cerius^2; and (c) Experimental peak data of anhydrous L-serine from ICDD

As described in Section 3.2.2.3, a Materials Visualizer program from Accelrys, Inc. was used to view the three-dimensional graphical model of L-serine molecules in its unit cell. The results are shown in Figure 4-17.

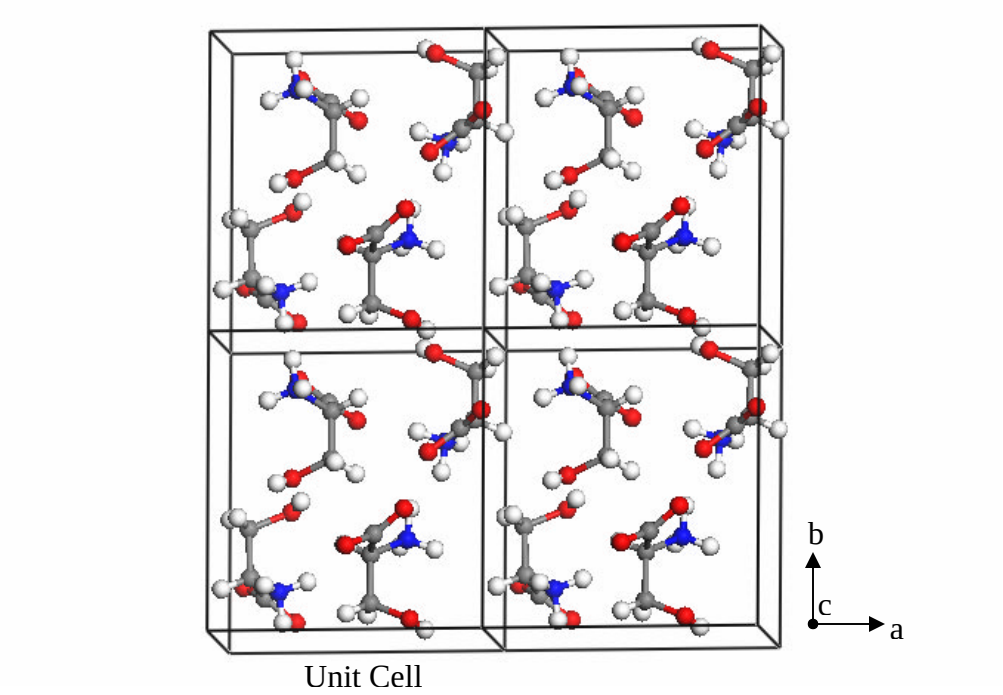

Figure 4-17: Crystal structure of anhydrous L-SER. Grey, red, white, and blue dots represent carbon, oxygen, hydrogen, and nitrogen atoms, respectively

4.2.2.2 L-serine Monohydrate Crystals

At the completion of each set of solubility measurements at a specific solvent composition, the temperature of the solution mixture is either around 5 ^{o}C or 10 ^{o}C (see Section 3.1.3). Optical microscopy has confirmed that the crystals at all solvent compositions studied appeared hexagonal at these temperatures. These crystals were analyzed with powder X-ray diffraction to confirm that they are the monohydrated from. Single-crystal data of L-serine monohydrate from Frey *et al*. (1973) were used to generate the calculated powder pattern using the program Cerius^{2}. This pattern was compared with the peak data collected from the powder X-ray diffractometer. The results are shown in Figure 4-18.

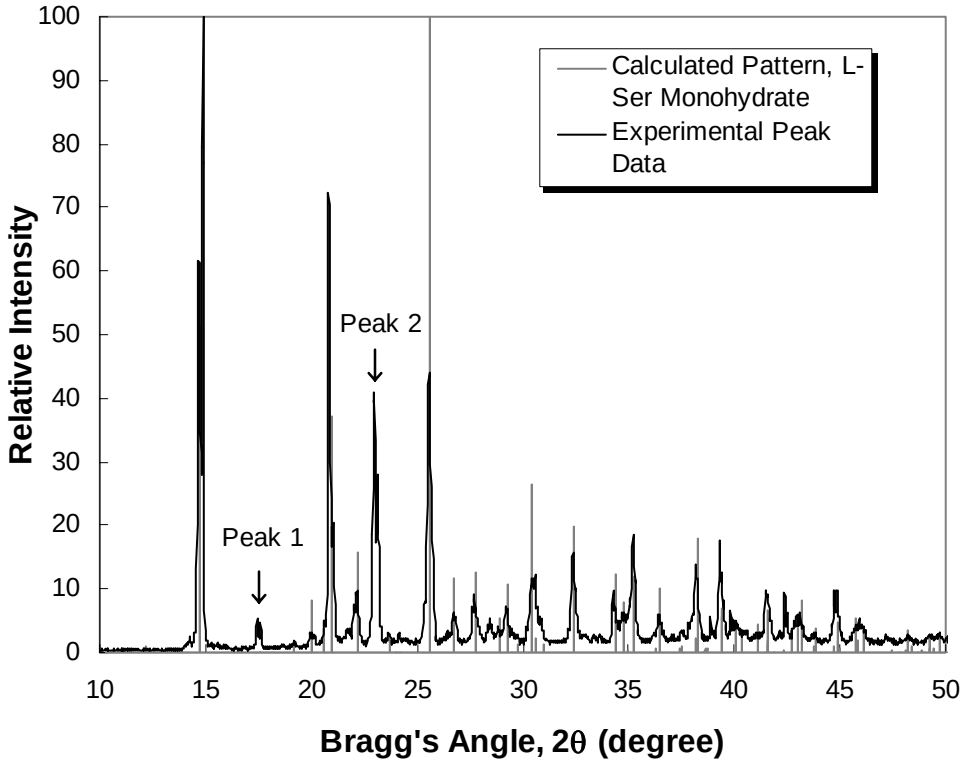

Figure 4-18: Comparison of the calculated powder pattern for L-serine monohydrate from Cerius[2] and the experimental powder pattern for the hexagonal L-serine crystals

All peak position in the experimental powder pattern agreed well with the calculated powder pattern with the exceptions of two peaks. They are highlighted and labeled Peak 1 and Peak 2 in Figure 4-18. Because of that, the experimental results are also compared with calculated powder pattern of anhydrous L-serine. This is shown in Figure 4-19.

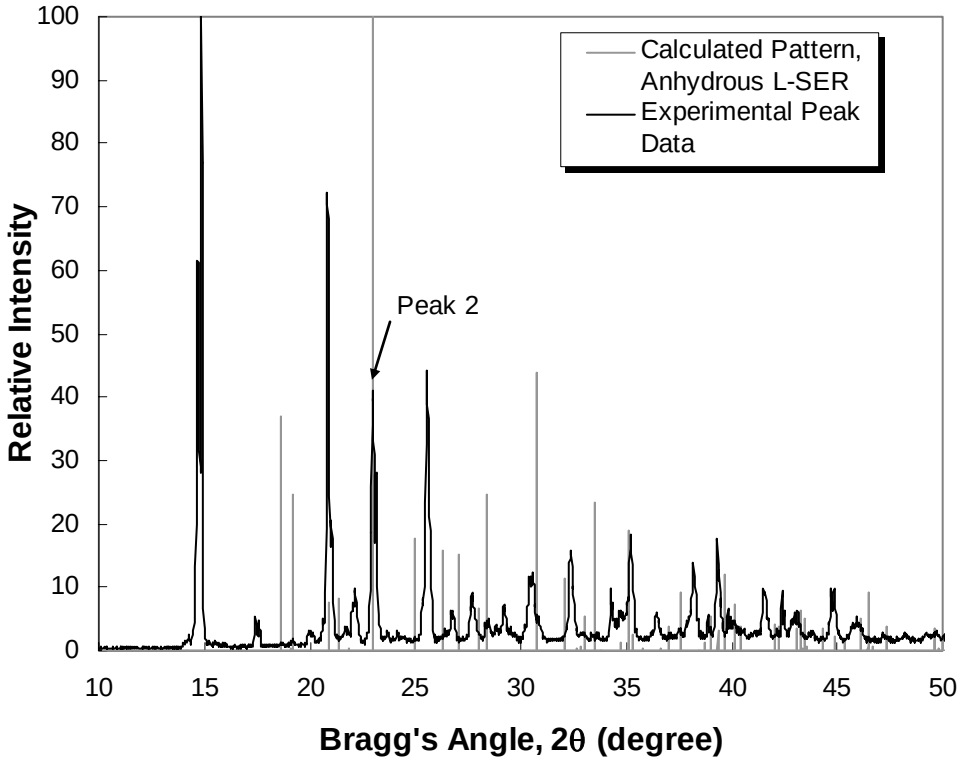

Figure 4-19: Comparison of the calculated powder pattern for anhydrous L-serine from Cerius[2] and the experimental powder pattern for the hexagonal L-serine crystals

The experimental peak pattern did not overlap with the calculated pattern of anhydrous L-serine, except at Bragg's Angle $2\theta = 22.96^{o}$. It corresponds to Peak 2 of Figure 4-25. Therefore, it is possible that trace amounts of L-serine monohydrate crystals were dehydrated. The origin of Peak 1 is still unknown. The powder pattern of the blank sample holder was collected and overlayed. In addition, the reported powder patterns of DL-serine, D-serine, methanol, L-tyrosine, L-alanine, and L-threonine (the impurities reported by Charmolue in L-serine from manufacturer) were compared. No peak was found to match that of Peak 1. But since Peak 1 only has a very low relative intensity, it is expected to be only a minor impurity peak. The high-degree of overlapping of the experimental peaks with the calculated pattern of L-serine monohydrate confirmed that

the vast majority of the powder crystals in the sample were indeed L-serine monohydrate crystals.

A graphical view of the unit cell of L-serine monohydrate is shown in Figure 4-20. L-serine molecules and water molecules are represented by the "ball and stick" convention and the "stick" convention respectively. It can be seen that each unit cell consists of four L-serine molecules and four water molecules.

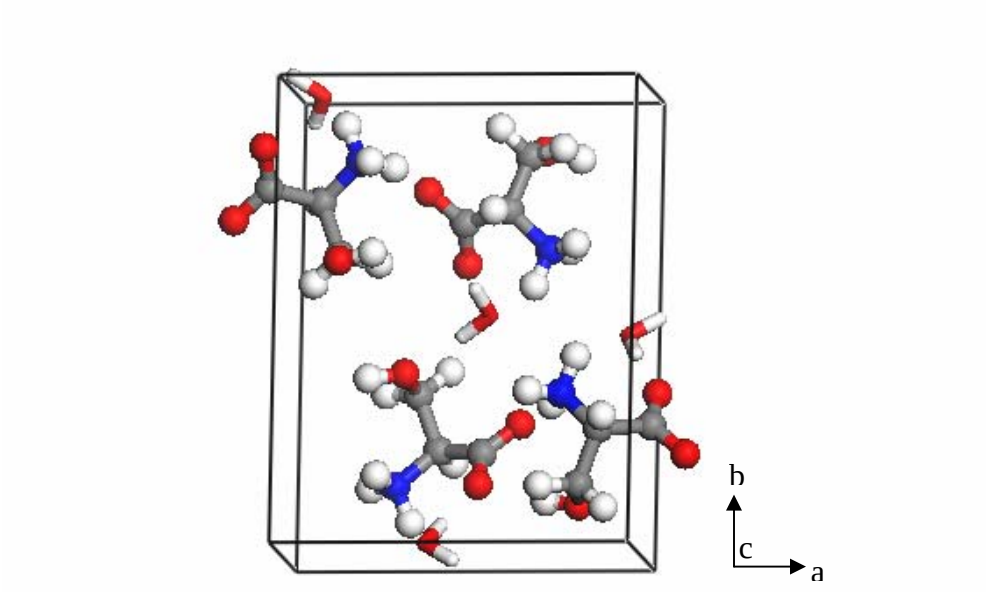

Figure 4-20: Crystal structure of L-SER·H_2O. The "ball and stick" convention is used for L-SER molecules, while the "stick" convention is used for water molecules. Grey, red, white, and blue labels represent carbon, oxygen, hydrogen, and nitrogen atoms, respectively

4.2.2.2.1 Dehydration of L-serine Monohydrate

As discussed in the previous section, the characterization of L-serine monohydrate crystals had presented challenges because of its possible solid-state transformation to the anhydrous form. In view of this, a drying method was adopted to study the process. A single crystal of L-serine monohydrate was isolated from the solution and placed on a glass slide. The initial morphology of the crystal was observed with an optical microscope. The slide was then placed in a desiccator and optical photomicrographs of the crystals were taken at certain time intervals. The sequence of transformation is presented in Figure 4-21.

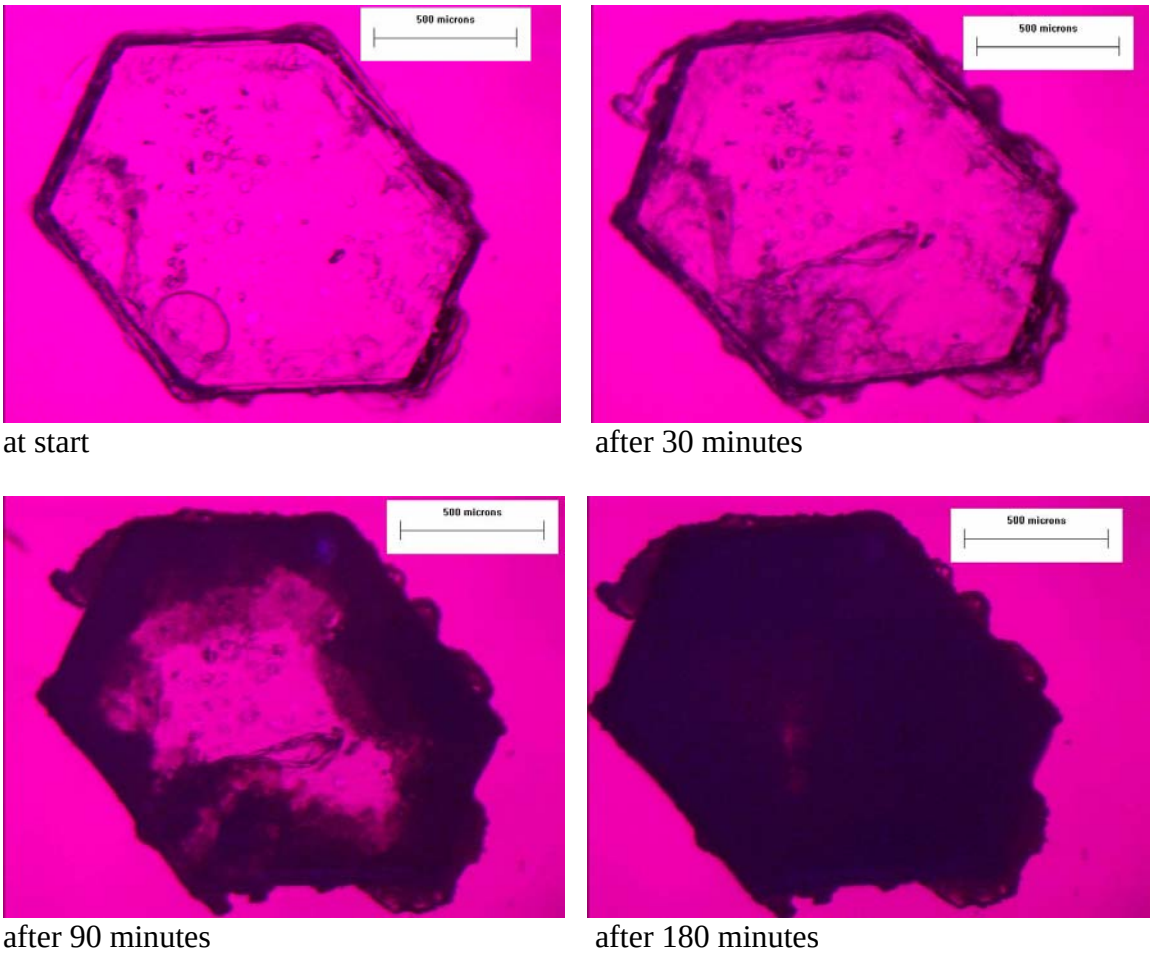

at start after 30 minutes

after 90 minutes after 180 minutes

Figure 4-21: Behavior of a L-serine monohydrate crystal in desiccator at ambient temperature

The crystal changed from transparent to opaque under transmitted light in just three hours. The darkening seemed to originate at the six edges of the crystal faces. Similar results were obtained in the dehydration of several pharmaceutical compounds in their solid-states (Byrn *et al*., 1999). It is suspected that L-serine monohydrate crystals transformed to the anhydrous form when they were separated from the solution.

To confirm the dehydration process, a series of powder X-ray diffraction data were collected with the L-serine monohydrate crystals as a function of time. The results are shown in Figure 4-22. The pattern at the bottom of the figure is the calculated

powder pattern of L-serine monohydrate, while the pattern on the top of the figure is the calculated powder pattern of anhydrous L-serine. The powder XRD pattern at t = 0 hr came from the same data collected for L-serine monohydrate crystals, as shown in Figures 4-18 and 4-19.

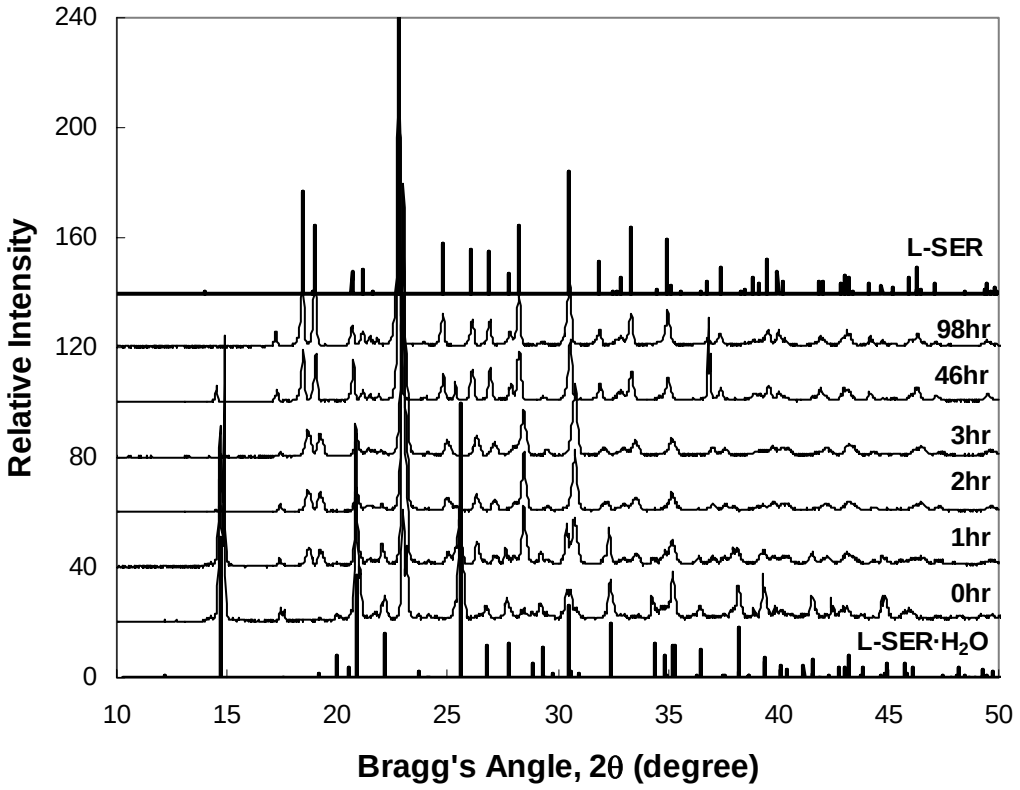

Figure 4-22: Powder XRD pattern for L-serine monohydrate crystals at times 0, 1, 2, 3, 46, and 98 hours. Pattern at the bottom is the calculated pattern of L-serine monohydrate; Pattern on the top is the calculated pattern of anhydrous L-serine

In general, the powder XRD pattern changed from resembling the monohydrate form to resembling the anhydrous form with time. For example, the peak with fairly high relative intensity at $2\theta = 14.72^{o}$ disappeared in the pattern at t = 98 hr, as there was no peak at that position for the anhydrous form. Also, two additional peaks were present between peak positions of 18^{o} and 20^{o} in the pattern at t = 1 hr and their relative intensities gradually increased with time. At t = 98 h, the peaks positions of these two peak matched with the pattern of anhydrous L-serine.

The dehydration process can be explained in terms of the placement of water molecules in the crystal lattice of L-serine monohydrate. A representative of the lattice structure of L-serine monohydrate is shown in Figure 4-23. In the unit cell, water molecules are next to other water molecules as channels along c-axis. This is consistent with the description of channel hydrates according to the classification of hydrates by Morris (1999). During the dehydration process, channels are formed when the water molecules leave the lattice structure. The lattice structure will collapse and new interactions are formed between L-serine molecules. This results in a transformation of the unit cell to the anhydrous form. Also, the single crystal of L-serine monohydrate changed from transparent to a white powder. Therefore, the single crystal appeared dark in Figure 4-21 under the transmitted light.

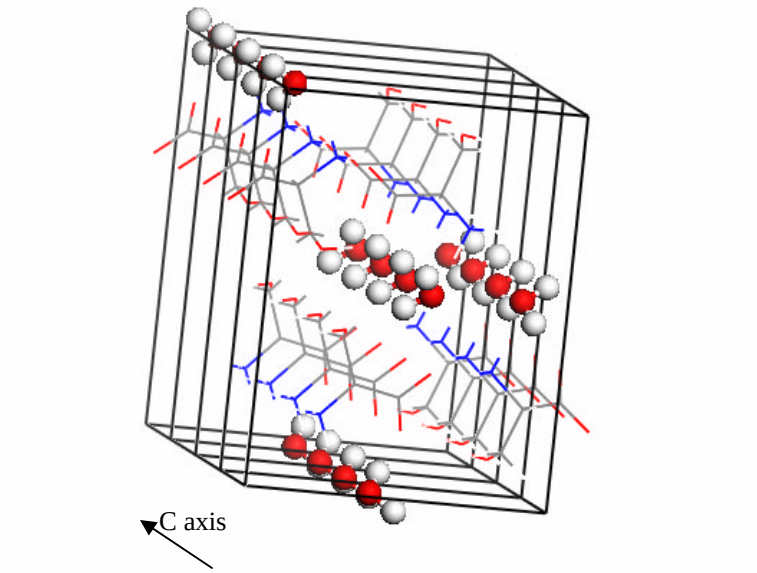

Figure 4-23: Water channels along the c-axis of the unit cell of L-serine monohydrate. To highlight the water molecules, a “ball and stick” convention is used. The L-serine molecules are presented by the “stick” convention. Grey, red, white, and blue labels represent carbon, oxygen, hydrogen, and nitrogen atoms, respectively

CHAPTER 5

CONCLUSIONS AND RECOMMENDATIONS

Solubilities of L-serine over a temperature range from 278 K to 333 K have been measured using high-performance liquid chromatography to determine equilibrium serine compositions in 0 mol%, 5 mol%, 10 mol%, 16 mol%, and 22 mol% methanol-in-water solutions. An increase in temperature was found to increase the solubility, while an increase in methanol concentration reduced the solubility drastically. The effect of methanol is more profound than the effect of temperature in the systems studied. When the solubility data were plotted as a function of temperature, empirical fits could be applied separately to solutions in equilibrium with hexagonal (monohydrate) L-serine crystals and to solutions in equilibrium with rod-shaped (anhydrous) crystals. The resulting graphs exhibited discontinuities corresponding to the transition in solid form. These fits could be extrapolated to connect at the transition point, thus identifying the conditions at which there was a transition between stable pseudo-polymorphs. This research is thought to be the first to report in the open literature the effect of methanol concentration in water on the temperature at which there was a transition from one stable species to another.

The solubility data have been correlated using the van't Hoff equation. The slope and intercept of the equation were used to estimate the enthalpy and entropy of solution, respectively. Enthalpy and entropy of solution were found to be of greater magnitude in L-serine monohydrate crystals than in anhydrous L-serine crystals. These values also increased with increase in methanol concentration. This is because L-serine was almost insoluble in methanol and therefore more energy was necessary in the dissolution process. Using the van't Hoff plots, the transition temperature for each water-methanol system was determined, and the transition temperature decreased in a non-linear fashion with increase in methanol concentration.

The morphology of L-serine crystals was examined using optical microscopy during the course of the solubility experiments. The crystals transformed from rod-like at high temperatures to hexagonal at lower temperatures. In addition, the rod-shaped (anhydrous) crystals adopted a more elongated shape at higher methanol concentration. The growth rate of the elongated faces was reduced relative to the growth rates of the other faces.

Structural analysis of L-serine was carried out using powder X-ray diffraction. The rod-shaped crystals were confirmed to be the anhydrous form, whereas the hexagonal were the monohydrated form. The monohydrate crystals started to dehydrate once they were removed from the solution. The dehydration phenomenon was observed in a single crystal of L-serine monohydrate and the change in powder pattern was recorded.

Recommendations for future research are listed as follows: liquid-phase activity coefficients can be obtained experimentally in mixed-solvent system in order gain insight

on the deviation from ideality. An isopiestic method is mentioned by Hutchens and co-workers (1963), and Kurosawa (2004) on such measurement. Since most activity coefficients for amino acids were measured at 25 ^{o}C, the dependence of temperature on activity coefficient can be explored further. These data can then be compared with those estimated from models for activity coefficients. As of now, the relationship between the morphology L-serine crystals and molecular packing in the unit cell is unknown. Studies by Berkovitch-Yellin (1985), Docherty and Roberts (1988), Clydesdale *et al*. (1991), Winn and Doherty (1998), and Givand *et al*. (1998) would be a good starting point on this subject.

APPENDIX A

Density Determination of Pure Methanol at 60 ^{o}C

Density of pure methanol at 60 ^{o}C was determined by a titration method. First, the temperature of the water circulator system was set to 60 ^{o}C. Pure methanol was added to a 100-mL glass bottle with screw cap (Pyrex brand media bottle, Catalog # 06-414-1A, Fisher Scientific). The bottle was immersed into the water circulator system and pre-heated. A 50-mL pipet and another 100-mL glass bottle were pre-heated to 60 ^{o}C in laboratory oven. Once pre-heated, the empty glass bottle was placed on a balance and tared. The pipet was connected to the pipet aid. Then, the bottle with pure methanol was removed from the water circulator, and 50-mL of the pure methanol was withdrawn and dispensed into the empty bottle on the balance. The mass of the solution was recorded. Density is calculated by dividing the mass of the pure methanol by its volume. The results are as followed:

Mass of Methanol (60 ^{o}C) = 38.0358 g

Volume of Methanol (60 ^{o}C) = 50 cm^{3}

Therefore,

Density of Methanol (60 ^{o}C) = 38.0358 g/50 cm^{3} = 0.7607 g/cm^{3}

APPENDIX B

HPLC Calibration Charts

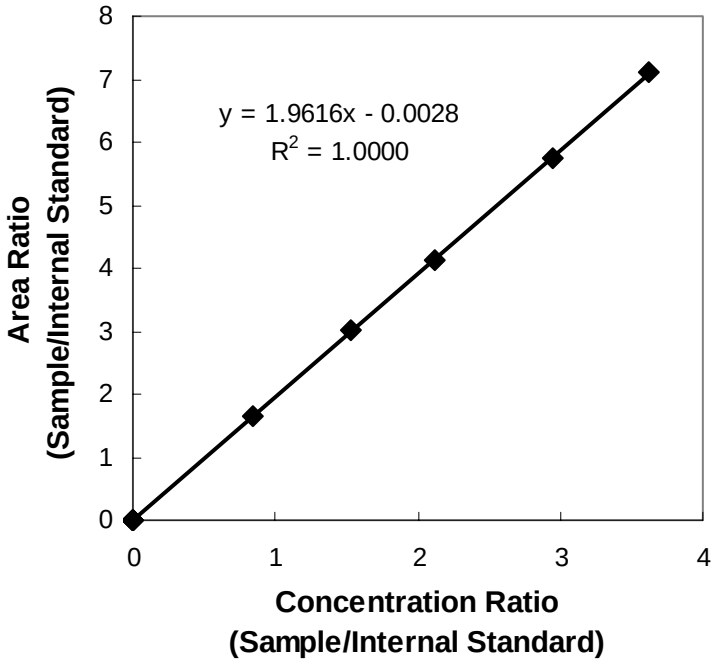

Figure B-1: Calibration chart #1

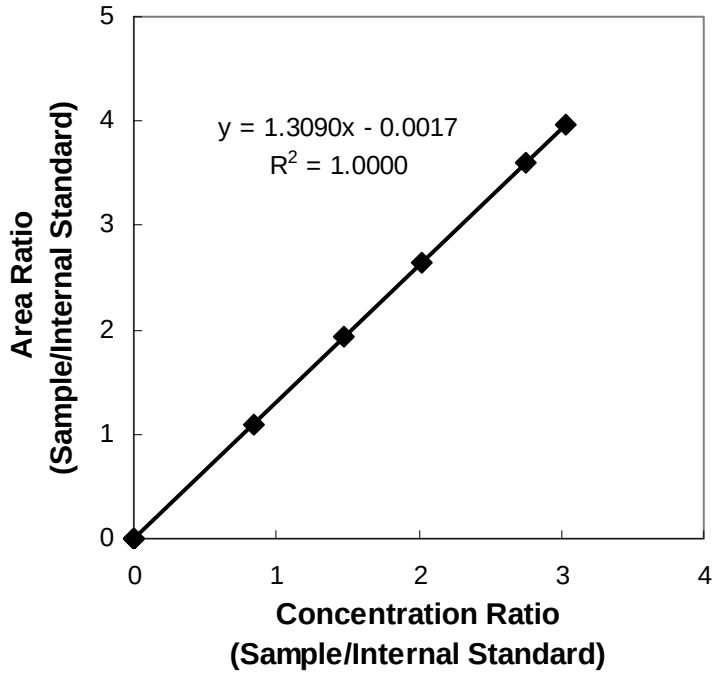

Figure B-2: Calibration chart #2

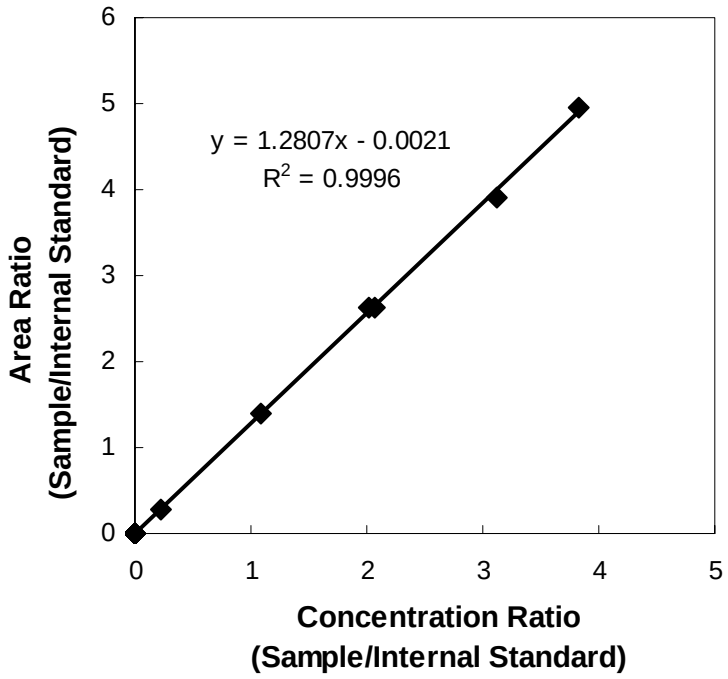

Figure B-3: Calibration chart #3

REFERENCES

Arii, K, Y. Kuniba, K. Tanimura, and Y. Fukuda, *Jpn. Kokai Tokkyo Koho*, Patent No. JP 06279290. "Nutritional Infusion Solutions Containing Fats, Glucose, Amino Acids, and Electrolytes," April 10, 1994

Beckmann, W., "Seeding the Desired Polymorph: Background, Possibilities, Limiatations, and Case Studies," *Organic Process Research & Development*, **4**, 372 (2000)

Beiny, D. H. M., and J. W. Mullin, "Solubilities of Higher Normal Alkanes in *m*-Xylene," *Journal of Chemical and Engineering Data*, **32**, 9 (1987)

Benedetti, E., C. Pedone, and A. Sirigu, "The Crystal Structure of L-Serine," *Gazzetta Chimica Italiana*, **103**, 555 (1973)

Berkovitch-Yellin, Z. "Toward an ab Initio Derivation of Crystal Morphology," *Journal of the American Chemical Society*, **107**, 8239 (1985)

Bernstein, J., R. J. Davey, and J. Henck, "Concomitant Polymorphs," *Angewandte Chemie*, **38**, 3441 (1999)

Bondi, A., *Physical Properties of Molecular Crystals, Liquids and Glasses*, Ch. 14, Wiley, New York (1968)

Brittain, H. G., *Polymorphism in Pharmaceutical Solids*, Marcel Dekker, New York (1999)

Byrn, S. R., R. R. Pfeiffer, and J. G. Stowell, 2nd Ed., *Solid-State Chemistry of Drugs*, SSCI, Inc., Indiana (1999)

Carozzo, L., G. Corongiu, and C. Petrongolo, "Analytical Potentials from ab initio Computations for the Interaction Between Biomolecules. IV. Water with Glycine and Serine Zwitterions," *Journal of Chemical Physics*, **68**, 787 (1978)

Charmolue, H, "The Effects of Process Variables on Purity, Size, and Habit of L-Serine Crystals Recovered by Batch Crystallization," M.S. Thesis, Georgia Institute of Technology (1990)

Charmolue, H, and R. Rousseau, "L-Serine Obtained by Methanol Addition in Batch Crystallization," *AIChE Journal*, **37**, 1121 (1991)

Chemburkar, S. R., J. Bauer, K. Deming, H. Spiwek, K. Patel, J. Morris, R. Henry, S. Spanton, W. Dziki, W. Porter, J. Quick, P. Bauer, J. Donaubauer, B. A. Narayanan, M. Soldani, D. Rilay, and K. McFarland, "Dealing with the Impact of Ritonavir Polymorphs on the Late Stages of Bulk Drug Process Development," *Organic Process Research & Development*, **4**, 413 (2000)

Chen, C. C., H. I. Britt, J. F. Boston, L. B. Evans, "Local Composition Model for Excess Gibbs Energy of Electrolyte System, 1: Single-Solvent, Single Completely Dissociated Electrolyte Systems," *AIChE Journal*, **21**, 444 (1982)

Chen, C. C., Y. Zhu, L. B. Evans, "Phase Partitioning of Biomolecules: Solubilities of Amino Acids," *Biotechnology Process*, **5**, 111 (1989)

Chikamatsu, Y., M. Ootani, and M. Inagaki, *Jpn. Kokai Tokkyo Koho*, Patent No. JP 06279227, "Discoloration-free Skin Preparations and Cosmetics Containing Amino Acids and Trehalose," October 4, 1994

Clydesdale, G., R. Docherty, and K. J. Roberts, "HABIT – A Program for Predicting the Morphology of Molecular Crystals," *Computer Physics Communications*, **64**, 311 (1991)

Cohn, E. J., McMeekin, T. L., Edsall, J. T., Weare, J. H., "Studies in the Physical Chemistry of Amino Acids, Peptides and Related Substances. II. The Solubility of α-amino acids in water and in alcohol-water mixtures, *Journal of American Chemical Society*, **56**, 2270 (1934)

Dalton, J. D. and C. L. A. Schmidt, "The solubilities of Certain Amino Acids in Water, the Densities of Their Solutions at Twenty-five Degrees, and the Calculated Heats of Solution and Partial Molal Volumes," *Journal of Biological Chemistry*, **103**, 549 (1933)

Dalton, J. D., and C. L. A. Schmidt, "The Solubilities of Certain Amino Acids and Related Compounds in Water, the Densities of Their Solutions at Twenty-Five Degrees, and the Calculated Heats of Solution and Partial Volumes. II," *Journal of Biological Chemistry*, **109**, 241 (1935)

Deng, Y., and B. Roux, "Hydration of Amino Acid Side Chains: Nonpolar and Electrostatic Contributions Calculated from Staged Molecular Dynamics Free Energy Simulations with Explicit Water Molecules," *Journal of Physical Chemistry B*, **108**, 16567 (2004)

Dey, B.P., and S. C. Lahiri, "Solubilities of Amino Acids in Different Mixed Solvents," *Indian Journal of Chemistry*, **25A**, 136 (1986)

Dey, B. P., and S. C. Lahiri, "Solubilities of Amino Acids in Methanol +Water Mixtures at Different Temperatures," *Indian Journal of Chemistry*, **27A**, 297 (1988)

Docherty, R., and K. J. Roberts, "MORANG – A Computer Program Designed to Aid in the Determination of Crystal Morphology," *Computer Physics Communications*, **51**, 423 (1988)

Dunn, M. S., and F. J. Ross, "Quantitative Investigations of Amino Acids and Peptides. IV. The Solubility of the Amino Acids in Water-Ethyl Alcohol Mixtures," *Journal of Biological Chemistry*, **125**, 309 (1938)

Dunn, M. S., F. J. Ross, and L. S. Read, "The Solubility of Amino Acids in Water," *Journal of Biological Chemistry*, **103**, 579 (1933)

Eyal, A. M., and E. Bressler, "Industrial Separation of Carboxylic and Amino Acids by Liquid Membranes: Applicability, Process Considerations, and Potential Advantages," *Biotechnology and Bioengineering*, **41**, 287 (1993)

Fasman, G. D., *Handbook of Biochemistry and Molecular Biology*, Vol I, 3rd Ed, CRC Press, Cleveland (1976)

Ferreira, L. A., E. A. Macedo, and S. P. Pinho, "Solubility of Amino Acids and Diglycine in Aqueous-Alkanol Solutions", *Chemical Engineering Science*, **59**, 3117 (2004)

Frey, M. N., M. S. Lehmann, T. F. Koetzle, and W. C. Hamilton, "Precision Neutron Diffraction Structure Determination of Protein and Nucleic Acid Components XI. Molecular Configuration and Hydrogen Bonding of Serine in the Crystalline Amino Acids L-Serine Monohydrate and DL-Serine," *Acta Crystallographica*, **B29**, 876 (1973)

Florey, K., "Cephradine," In: Florey, K. (Ed), *Analytical Profiles of Drug Substances* Academic Press, New York, Vol. 2, 1 (1973)

Gatewood, M. D., Solubility and Recovery of L-Isoleucine from High pH Solutions, and The Cause for L-serine Habit Differences When Crystallized from Water and Methanol/Water Solutions," M.S. Thesis, Georgia Institute of Technology (1992)

Gekko, K., "Mechanism of Polyol-induced Protein Stabilization: Solubility of Amino Acids and Diglycine in Aqueous Polyol Solution," *Journal of Biochemistry*, **90**, 1633 (1981)

Ghotbi, C., and J. H Vera, "Extension to Mixtures of Two Robust Hard-Sphere Equations of State Satisfying the Ordered Close-Packed Limit", *Canadian Journal of Chemical Engineering*, **79**, 678 (2001)

Giron, D., "Thermal Analysis and Calorimetric Methods in the Characterization of Polymorphs and Solvates," *Thermochimica Acta*, **248**, 1 (1995)

Givand, J. C., R. W. Rousseau, and P. J. Ludovice, "Chacterization of L-Isoleucine Crystal Morphology from Molecular Modeling," *Journal of Crystal Growth*, **194**, 228 (1998)

Goodfellow, J. M., J. L. Finney, and P. Barnes, "Monte Carlo Computer Simulation of Water-Amino Acid Interactions," *Proceedings of the Royal Society of London, Series B: Biological Sciences*, **214**, 213 (1982)

Goto, S., and T. Isemura, "Studies of the Hydration and the Structure of Water and Their Roles in Protein Structure. IV. The Hydration of Amino Acids and Oligopeptides," *Bulletin of the Chemical Society of Japan*, **37**, 1697 (1964)

Grant, D. J. W., "Theory and Origin of Polymorphism," In: Brittain, H. G. (Ed), *Polymorphism in Pharmaceutical Solids*, Marcel Dekker, New York, 1 (1999)

Grant, D. J. W., and C. H. Gu, "Estimating the Relative Stability of Polymorphs and Hydrates from Heats of Solution and Solubility Data," *Journal of Pharmaceutical Sciences*, **90**, 1277 (2001)

Greenberg, D. A., C. D. Barry, and G. R. Marshall, "Investigation and Parametrization of a Molecular Dielectric Function," *Journal of the American Chemical Society*, **100:13**, 4020 (1978)

Griesser, U. J., A. Burger, and K. Mereiter, "The Polymorphic Drug Substances of the European Pharmacopoeia. Part 9. Physiochemical Properties and Crystal Structure of Acetazolamide Crystal Forms," *Journal of Pharmaceutical Sciences*, **86**, 352 (1997)

Gude, M. T., H. H. J. Meuwissen, L. A. M. Wielen, and K. Ch. A. M. Luyben, "Partition Coefficients and Solubilities of α-Amino Acids in Aqueous 1-Butanol Solutions," *Industrial and Engineering Chemistry Research*, **35**, 4700 (1996a)

Gude, M. T., L. A. M. van der Wielen, and K. Ch. A. M. Luyben, "Phase Behavior of z-Amino Acids in Multicomponent Aqueous Alkanol Solutions," *Fluid Phase Equilibria*, **116**, 110 (1996b)

Gupta, R. B., and R. A. Heidemann, "Solubility Models for Amino Acids," *AIChE Journal*, **36**, 333 (1990)

Gusev, Yu. A., Y. F. Zuev, and N. V. Sedykh, "Study of Amino Acid Hydration Using Dielectric Measurements and EPR Spin Labeling," Abstract: *Tezisy Dokl. - Vses. Konf. Spektrosk. Biopolim., 2nd*, **38** (1974)

Haisa, M., S. Kashino, R. Kawai, and H. Maeda, "The Monoclinic Form of p-Hydroxyacetanilide," *Acta Crystallographica*, **B32**, 1283 (1976)

Haisa, M., S. Kashino, and H. Maeda, "Orthorhombic Form of p-Hydroxyacetanilide," *Acta Crystallographica*, **B30**, 2510 (1974)

Hayden, P. J., and V. S. Goldman, *U.S. Patent No. 6,060,043*, "Deodorant Composition Containing D-Amino Acid," May 9, 2000

Hill, D. W., F. H. Walters, T. D. Wilson, and J. D. Stuart, "High Performance Liquid Chromatographic Determination of Amino Acids in the Picomole Range," *Analytical Chemistry*, **51**, 1338 (1979)

Hollenberg, J. L., and J. B. Ifft, "Hydration Number by Near-Infrared Spectrophotometry. 1. Amino Acids," *Journal of Physical Chemistry*, **86**, 1938 (1982)

Hou, J. P., and J. W. Poole, "Amino Acid Nature of Ampicillin and Related Penicillins," *Journal of Pharmaceutical Sciences*, **58**, 1510 (1969)

Hutchens, J. O., K. M. Figlio, and S. M. Granito, "An Isopiestic Comparison Method for Activities," *The Journal of Biological Chemistry*, **238**, 1419 (1963)

Jeffrey, G. A., and J. Mitra, "Three-Center (Bifurcated) Hydrogen Bonding in the Crystal Structures of Amino Acids," *Journal of the American Chemical Society*, **106**, 5546 (1984)

Jozwiakowski, M. J., N. T. Nguyen, J. M. Sisco, and C. W. Spancake, "Solubility Behavior of Lamivudine Crystal Forms in Recrystallization Solvents," *Journal of Pharmaceutical Sciences*, **85**, 193 (1996)

Khankari, R. K., D. J. W. Grant, "Pharmaceutical Hydrates," *Thermochimica Acta*, **248**, 61 (1995)

Khoshkbarchi, M. K., and J. H. Vera, "A Simplified Perturbed Hard-Sphere Model for the Activity Coefficients of Amino Acids and Peptides in Aqueous Solutions," *Industrial & Engineering Chemistry Research*, **35**, 4319 (1996)

Khoshkhoo, S., and J. Anwar, "Crystallization of Polymorphs: the Effect of Solvent," *Journal of Physics. D, Applied Physics*, **26**, B90 (1993)

Kim, T. K., and M. S. Jhon, "Theoretical Study on the Water Structure of the Aqueous Amino Acid Solutions Using Monte Carlo Method," *Journal of Molecular Liquids*, **59**, 179 (1994)

Kistenmacher, T. J., G. A. Rand, and R. E. Marsh, "Refinements of the Crystal Structure of DL-Serine and Anhydrous L-Serine", *Acta Crystallographica*, **B30**, 2573 (1974)

Kobayashi, H., *U.S. Patent No. 6,620,967*, "Therapeutic Agents for Controlling Ketosis," September 16, 2003

Koichi, H., N. Nobuya, and T. Hino, "Water of Crystallization of Amino Acids and Their Salts," Abstract: *Nippon Nogeikagaku Kaishi*, **38**, 77 (1964)

Kotova, D. L., O. A. Vinogradova, L. M. Kalinina, "Specific features of hydration of aliphatic amino acids," Abstract: *Zhurnal Fizicheskoi Khimii*, **76**, 2247 (2002)

Kubota, K., and K. Yokozeki, "Production of L-serine from Glycine by Corynebacterium and Properties of Serine Hydroxymethyltransferase, a Key Enzyme in L-serine production," *Journal of Fermentation and Bioengineering*, **67**(6), 387 (1989)

Kunioka, M, "Biodegradable Water Absorbant Synthesized from Bacterial Poly(amino acid)s," *Macromolecular Bioscience*, **4**, 324 (2004)

Kusumoto, I, "Glutamine Metabolism: Nutritional and Clinical Significance," *The Journal of Nutrition*, **9S**, 2552S (2001)

Lafferrère, L., C. Hoff, and S. Veesler, "Polymorphism and Liquid-Liquid Demixing in Supersaturated Drug Solution," *Engineering in Life Sciences*, **3**, 127 (2003)

Larson, B. L., P. Rasmussen, and A. Fredenslund, "A Modified UNIFAC Group-Contribution Model for Prediction of Phase Equilibria and Heat of Mixing," *Industrial & Engineering Chemistry Research*, **26**, 2274 (1987)

Martino, P. Di, A.-M., Guyot-Hermann, P. Conflant, M. Drache, J.-C.Guyot, "A New Pure Paracetamol for Direct Compression: the Orthorhombic Form," *International Journal of Pharmaceutics*, **128**, 1 (1996)

Maruyama, S., H. Ooshima, "Mechanism of the Solvent-mediated Transformation of Taltirelin Polymorphs Promoted by Methanol," *Chemical Engineering Journal*, **81**, 1 (2001)

Mazer, T. B., A. Marchio, and P. Acosta, *U.S. Patent No. 2004213838*. "Medical Food Tablets Containing Free Amino Acids," October 28, 2004

McMeekin, T. L., E. J. Cohn, J. H. Weare, "Studies in the Physical Chemistry of Amino Acids, Peptides, and Related Substances. III. The Solubility of Derivatives of the Amino Acids in Alcohol-water Mixtures," *Journal of American Chemical Society*, 57, **626** (1935)

Mitchell, A. G., "Polymorphism in Metochlopramide and Metochlopramide Hydrochloride," *Journal of Pharmacy and Pharmacology*, **37**, 601 (1985)

Morris, C. E., B. J. Trask-Morrell, N. M. Morris, and S. L. Batiste, "Aqueous Solubility, Polymorphism, and Pseudopolymorphism of meso-1,2,3,4-Butanatetracarboxylic Acid," *Industrial & Engineering Chemistry Research*, **43**, 5347 (2004)

Morris, K. R., "Structural Aspects of Hydrates and Solvates," In: Brittain, H. G. (Ed), *Polymorphism in Pharmaceutical Solids*, Marcel Dekker, New York, 125 (1999)

Mortazavi-Manesh, S., C. Ghotbi, and V. Taghikhani, "A New Model for Predicting Activity Coefficients in Aqueous Solutions of Amino Acids and Peptides," *Journal of Chemical Thermodynamics*, **35**, 101 (2003)

Mullin, J. W., *Crystallization*, 4th Ed., Butterworth-Heinemann, MA (2001)

Naim, M, I. Ohara, M. R. Kare, and M. Levinson, "Interaction of MSG taste with nutrition: Perspectives in Consummatory Behavior and Digestion," *Physiology and Behavior*, **49**, 1019 (1991)

Nagao, S., and K. Uehara, "Application to the Cosmetics of Amino Acid Derivatives," *Fragrance Journal*, **32**, 51 (2004)

Nass, K. K., "Representation of the Solubility Behavior of Amino Acids in Water," *AIChE Journal*, **34** (8), 1257 (1988)

Nozaki, Y., and C. Tanford, "The Solubility of Amino Acids and Two Glycine Peptides in Aqueous Ethanol and Dioxane Solutions," *Journal of Biological Chemistry*, **246**, 2211 (1971)

Obst, M, and A. Steinbüchel, "Microbial Degradation of Poly(amino acid)s," *Biomacromolecules*, **5**, 1166 (2004)

O'Connell, J. P., "Molecular Thermodynamics of Gases Solubility in Mixed Solvents," *AIChE Journal*, **17**, 659 (1971)

O'Connell, J. P, and J. M. Prausnitz, "Thermodynamics of Gas Solubility in Mixed Solvents," *Industrial and Engineering Chemistry Fundamentals*, **3**, 347 (1964)

Orella, C. J., and D. J. Kirwan, "The Solubility of Amino Acids in Mixtures of Water and Aliphatic Alcohols," *Biotechnology Progress*, **5**, 89 (1989)

Orella, C. J., and D. J. Kirwan, "Correlation of Amino Acid Solubilities in Aqueous Aliphatic Alcohol Solutions," *Industrial and Engineering Chemistry Research*, **30**, 1040 (1991)

Perry's Chemical Engineer's Handbook, McGraw-Hill Companies, Inc. (1999)

Pinho, S. P., C. M. Silva, and E. A. Macedo, "Solubility of Amino Acids: A Group-Contribution Model Involving Phase and Chemical Equilibria," *Industrial & Engineering Chemistry Research*, **33**, 1341 (1994)

Pitzer, K. S., "Electrolytes. From Dilute Solutions to Fused Salts," *Journal of American Chemical Society*, **102**, 2902 (1980)

Pominov, I. S., D. R. Sidorova, and B. P. Khalepp, "Hydration of Amino Acids," Abstract: *Zhurnal Strukturnoi Khimii*, **13**, 1084 (1972)

Prausnitz, J. M., R. N. Lichtenthaler, and E. G. de Azevedo, *Molecular Thermodynamics of Fluid-Phase Equilibria*, 3rd Ed., Prentice Hall PTR, New Jersey (1999)

Roth, M., "Fluorescence Reaction for Amino Acids," *Analytical Chemistry*, **43** (7), 880 (1971)

Roweton, S., S. J. Huang, and G. Swift, "Poly(aspartic acid): synthesis, biodegradation, and current applications," *Journal of Environmental Polymer Degradation*, **5**(3), 175 (1997)

Seddon, K. R., "Crystal Engineering: A Case Study," *NATO ASI Series, Series C: Mathematical and Physical Sciences*, **539** (Crystal Engineering: The Design and Application of Functional Solids), 1 (1999)

Sidorova, D. R., I. S. Pominov, and B. P. Khalepp, "Experimental Confirmation of Amino Acid Hydration Model," Abstract: *Aspir. Rab., Kazon. Gos. Univ., Tochnye Nauki: Mekh., Fiz.*, 141 (1971)

Suzuki, T., T. Hasegawa, and N. Matsumoto, "Hair Lotion Containing Acetylmethionine and Serine," *Jpn. Kokai Tokkyo Koho*, Patent No. JP 49000451, January 5, 1974

Threlfall, T. "Crystallization of Polymorphs: Thermodynamic Insight into the Role of Solvent," *Organic Process Research & Development*, **4**, 384 (2000)

Taichibana, Y., M. Kurisawa, H. Uyama, T. Kakuchi, and S. Kobayashi, " Biodegradable Thermoresponsive Poly(Amino acid)s," *Chemical Communications*, **1**, 106 (2003)

Vorob'ev, M. M., A. A. Baranov, V. M. Belikov, and Y. I. Khurgin, "The Investigation of α-Amino Acid Hydration by Absorption Millimeter Spectroscopy," Abstract: *Izvestiya Akademii Nauk, Seriya Khimicheskaya*, **3**, 618 (1996)

Winn, D., and M. F. Doherty, "A New Technique for Predicting the Shape of Solution-Grown Organic Crystals," *AIChE Journal*, **44**, 2501 (1998)

Yamauchi, K., T. Ogawa, T. Katsura, and K. Kuniba, *Jpn. Kokai Tokkyo Koho*. Patent No. JP 2003252757. "Preparation of Intravenous Infusion of Drug Delivery System," September 10, 2003.